Journal of Structural Geology 190 (2025) 105294

Contents lists available at ScienceDirect

Journal of Structural Geology

journal homepage: www.elsevier.com/locate/jsg

# Studying the kinematics of magma emplacement in fabric-weak, epizonal plutons: The example of the Sauce Guacho and Santa Rosa plutons, eastern Sierras Pampeanas, Argentina

Ana Eugenia Acosta-Nagle [a], Juan Díaz-Alvarado [b,*], Carlos Fernández [c], Rodolfo Christiansen [d], Fernando Javier D'Eramo [e], Lucio Pedro Pinotti [e], José Pablo López [a], Laura Iudith Bellos [a]

[a] INSUGEO-CONICET, Facultad de Ciencias Naturales e IML, UNT, Miguel Lillo 205, CP 4000, San Miguel de Tucumán, Argentina
[b] Departamento de Biología y Geología, Física y Química Inorgánica, ESCET, Universidad Rey Juan Carlos, 28933, Móstoles, Spain
[c] Departamento de Geodinámica, Estratigrafía y Paleontología, Facultad de Ciencias Geológicas, Universidad Complutense de Madrid, 28040, Madrid, Spain
[d] Leibniz Institute for Applied Geophysics (LIAG), Stilleweg 2, 30655, Hanover, Germany
[e] Instituto de Ciencias de la Tierra, Biodiversidad y Ambiente (ICBIA) (UNRC-CONICET), Departamento de Geología, Facultad de Ciencias Exactas Físico-Químicas y Naturales, Universidad Nacional de Río Cuarto, Ruta Nacional 36 Km 601, (X5804BYA) Río Cuarto, Córdoba, Argentina

ARTICLE INFO

*Keywords:*
Upper crustal plutons
Emplacement mechanism
Geophysical imaging
Structural analysis
Intracontinental magmatism
Eastern sierras pampeanas

ABSTRACT

This work presents emplacement kinematics for two plutons emplaced in a crustal level dominated by brittle conditions as a useful methodology in the study of shallow, small intrusive bodies where the field evidence of deformation is scarce.

The study was carried out in the Sauce Guacho and Santa Rosa plutons, both located on NO sector of Sierra de Ancasti. They are zoned syeno-monzogranitic, strongly peraluminous intrusive bodies representing typical Carboniferous intracontinental magmatism in the Eastern Sierras Pampeanas of Argentina. Both plutons present ellipsoidal external shapes, and sharp and discordant contacts with the host rocks suggesting an emplacement with high rheological contrast between the intrusive magma and the metamorphic host rock. The geophysical study highlights an elongated, arcuate gravimetric low that coincides and is aligned with the long axis of both plutons and with a zone characterized by brittle structures. Regarding structural measurements, the main penetrative structure of the host rocks (Ancasti Formation) shows an averaged NNW-SSE orientation and presents a slight but significant variation close to the plutons. Magmatic fabrics were observed in the porphyritic units (K-feldspar megacrysts) that constitute part of the igneous bodies. All these pieces of evidence suggest a possible structural control during the emplacement of the igneous bodies and constitute the data used in the structural analysis that tests five different conceptual models simulating the shear zone influence for the emplacement of the plutons.

According to our kinematic analysis, the distinct structural features and external shapes found in the Sauce Guacho and Santa Rosa plutons and their metamorphic envelope were imposed by the curved deformation zone. Thus, magma ascent and emplacement were probably assisted by the nucleation and growth of a dextral transtensional structure, with a predominance of simple shear ($Wk \gg 0.81$) in its southern, NNE-SSW-striking segment (Santa Rosa pluton area), and with a predominance of pure shear ($0.6 > Wk > 0.1$) in its northern, NE-SW striking segment (Sauce Guacho pluton area).

In addition to a feasible emplacement model, our structural analysis shed light on the barely known Carboniferous tectonic scenario in this intracontinental setting of SW Gondwana. The common divergence angle estimated for both brittle-ductile shear zone segments is oriented $157° \pm 9°$. Therefore, this structure could have acted as a dextral transtensional structure with predominance of the coaxial component (extension) in NE-SW segments and dominated by simple shear in oblique NNE-SSW branches, interpreted as R-type fractures.

* Corresponding author.
*E-mail address:* juan.diaz@urjc.es (J. Díaz-Alvarado).

https://doi.org/10.1016/j.jsg.2024.105294
Received 19 September 2024; Received in revised form 15 November 2024; Accepted 15 November 2024
Available online 19 November 2024

## 1. Introduction

Studies about kinematics and strain in combination with fluid mechanics allowed geologists to expand the knowledge about the ascent and emplacement mechanisms involved in the construction of igneous bodies. The upward migration of magmas and the batholith building are linked to deformation affecting crustal host rocks, as an interaction between magma buoyancy and regional tectonics stress, where both magmatism and tectonic deformation are part of the same process (Brun and Pons, 1981; Hutton, 1988, 1997; Bouchez, 1997; de Saint-Blanquat et al., 1998; Vigneresse, 2004). The understanding of geodynamic settings and regional syn-magmatic kinematics, especially in the case of

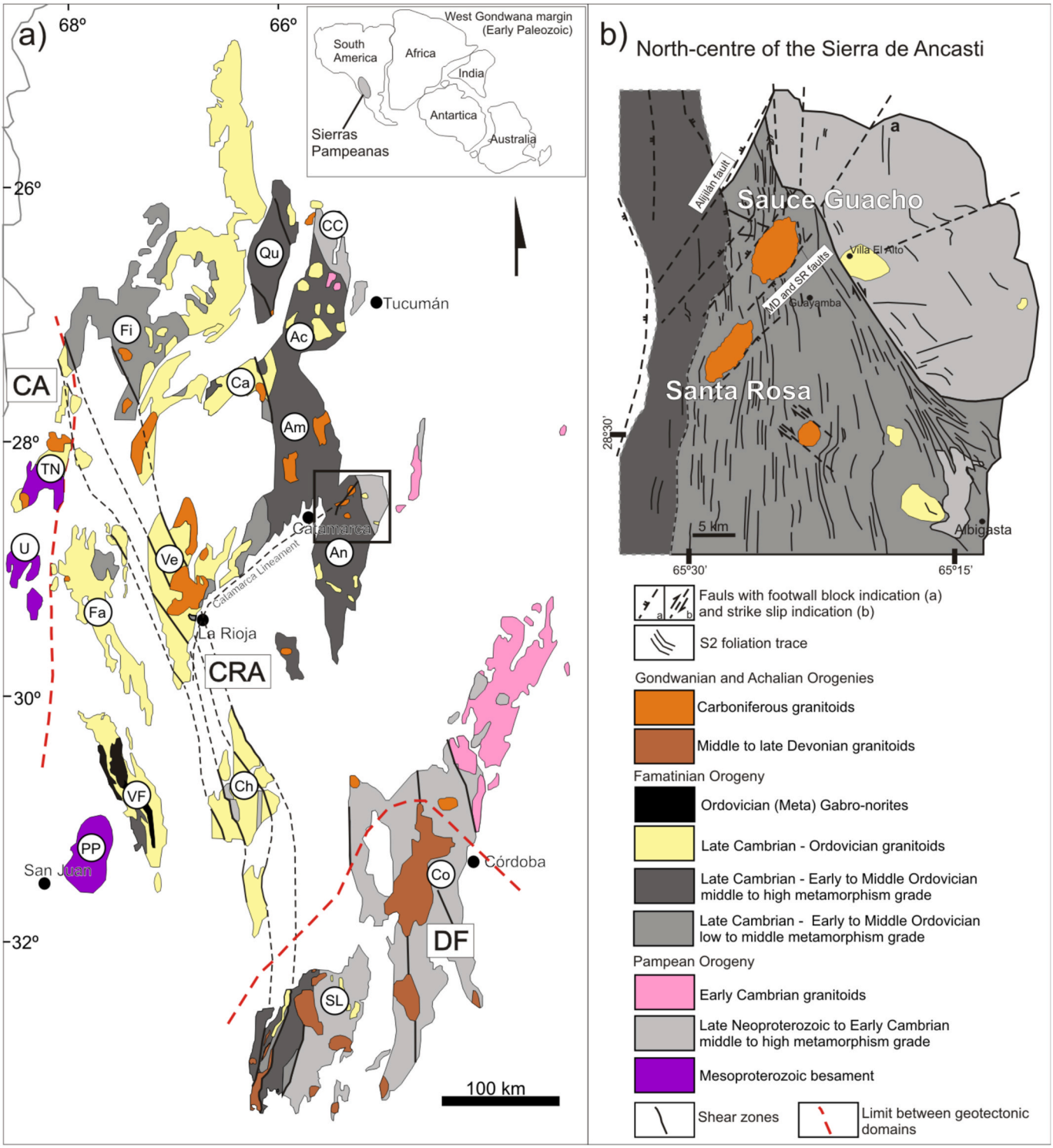


**Fig. 1.** a) Geological sketch of central and NW Argentina. Geotectonic domains are indicated: Devonian Foreland (DF), Carboniferous Arc (CA) and Carboniferous Retro-Arc (CRA). Shear zones (black line) and its prolongation (black line-cut) are indicate. Abbreviations ranges: SL (San Luis), Co (Córdoba), Ch (Chepes), VF (Valle Fértil), PP (Pié de Palo), An (Ancasti), Am (Ambato), Ve (Velasco), Fa (Famatina), CC (Cumbres Calchaquíes), Ac (Aconquija), Ca (Capillitas), Qu (Quilmes), Fi (Fiambalá), TN (Toro Negro), U (Umango). b) North-central Sierra de Ancasti (Sierra Brava Complex: gray light; Ancasti Formation: medium gray; El Portezuelo Ígneo-Metamórphic Complex: dark gray). MD: Mina Dal fault. SR: Santa Rosa fault.

small plutons, is not always clear. These studies are grounded in a petrological and structural analysis of igneous bodies and their associated host rocks. This analysis aims to elucidate the degree of interaction between magmatic forces and tectonic processes, thereby facilitating the development of emplacement models (Bouchez et al., 1981; Guillet et al., 1985; Aranguren et al., 1996; Bouchez, 1997; Aranguren et al., 1997; Hutton, 1988; Vegas et al., 2001; Pinotti and D'Eramo, 2008; de Saint-Blanquat et al., 2011).

In the shallow crust, the emplacement mechanisms are mostly associated with extensional structures in shear systems which may operate in a complex linked network of fault planes and zones, where diking is the most efficient magma migration mechanism (Hutton, 1988, 1992; Vigneresse, 1995; de Saint Blanquat et al., 1998; Clemens, 1998; Tobish and Paterson, 1990; Hutton et al., 1990; Guillet et al., 1985; Hutton and Reavy, 1992; Clemens and Mawer, 1992; Petford et al., 2000; Marcotte et al., 2005). However, these structures are not always easy to observe. In some cases, these structures are buried and only evidenced by the location of igneous bodies associated with minor structures (Vegas et al., 2001). In other cases, in upper-crustal levels, the brittle-ductile shear zones may be related to the development of mylonites, cataclastic zones, fault gouge, tectonic breccias or phyllonites (Tommasi et al., 1994; Aranguren et al., 1997; Vegas et al., 2001; Oriolo et al., 2024). At the same time, the presence of magmatic and/or solid-state fabrics in igneous bodies related to these structures also depends on the crystallization and cooling rate at the shallow emplacement level, which are expected to be fast processes in the case of small granitic bodies due to the great thermal contrast between the host rock and the melt (Castro, 1986; Bouchez et al., 1992; Aranguren et al., 1997; de Saint Blanquat et al., 2011; Díaz-Alvarado et al., 2012). Therefore, in some cases, it becomes complex to determine the location and orientation of the extensional structures that functioned as feeder channels or emplacement sites of the igneous bodies and thus, the kinematics of the structure that allowed its emplacement.

In this work, we present a feasible emplacement model for two plutons emplaced at reactivated deformation zones in a shallow crustal domain dominated by brittle-ductile conditions. The fact that there is little record of emplacement dynamics and tectonic deformation does not mean the uncoupling between the emplacement process and the host rock deformation, proposing in some cases rapid rates of tectonic deformation in relation to the emplacement of small bodies (e.g., Petford et al., 2000). This study aims to shed light on these questions and advance the understanding of the kinematics of the shear zone that we propose is associated with the emplacement of these granitic bodies. In this way, we show a useful methodology to study shallow plutons with weakly developed fabrics where the field evidence of deformation is scarce.

## 2. Geological setting

The study area is located at the northern tip of the Sierra de Ancasti mountain range, which is part of the Eastern Sierras Pampeanas, in the Northwest of Argentina (Fig. 1). In this sector crop out the Sauce Guacho (346–366 Ma, LA-ICP-MS U-Pb in apatite, Sardi et al., 2023), and Santa Rosa (336 ± 8 Ma, SHRIMP U-Pb in zircon, Dahlquist et al., 2018) plutons as a product of the intracontinental magmatism, coeval with arc magmatism developed to the west, that occurred continuously between 395 and 300 Ma (e.g., Alasino et al., 2012; Dahlquist et al., 2021; Alasino et al., 2022; Acosta-Nagle et al., 2022) (Fig. 1). It was characterized by Devonian batholithic intrusions in the southeastern sector of the Eastern Sierras Pampeanas (foreland setting) and Carboniferous small to medium-sized plutons and dykes in the central and northwestern sectors of this region (retro-arc and arc settings). It presents predominantly monzogranitic to syenogranitic compositions, comprising high to moderate peraluminous, calc-alkalic to alkali-calcic and high-K to shoshonitic magmatic series (Lira and Kirschbaum, 1990; Llambías et al., 1998; Grosse and Sardi, 2005; Grosse et al., 2009; López de Luchi et al., 2017; Dahlquist et al., 2010, 2013, 2021; Toselli et al., 2011, 2014; Alasino et al., 2012; Acosta Nagle and López, 2014; Báez et al., 2018; Acosta Nagle et al., 2022). Isotopic signatures are typical of mixing of old crustal (meta-sedimentary and igneous) and juvenile components, the later increasing to the west (Grosse et al., 2009; Alasino et al., 2012; López de Luchi et al., 2017; Dahlquist et al., 2021; Acosta Nagle et al., 2022). This magmatism is characterized by emplacement in shallow crustal levels that were associated with a set of NNW- and NNE-trending shear zones of Cambrian, Ordovician, Devonian and Carboniferous age (Pinotti et al., 2002, 2006; López de Luchi et al., 2012; Alasino et al., 2012; Macchioli Grande et al., 2019; Acosta Nagle et al., 2022). An extensional/transtensional tectonic regime has been proposed for the Carboniferous in the study area (Stuart-Smith et al., 1999; Siegesmund et al., 2004; Pinotti et al., 2002; Pinotti et al., 2006; Grosse et al., 2009; Dahlquist et al., 2010, 2018, 2021; Toselli et al., 2014; Toselli and Rossi de Toselli, 2018; López de Luchi et al., 2012; Alasino et al., 2012; Macchioli Grande et al., 2019; Acosta Nagle et al., 2022).

The host rocks of the studied plutons correspond to the Ancasti Metamorphic Complex (Knüver and Reissinger, 1981; Miró et al., 2004; Verdechia et al., 2012): a succession of schists (Ancasti Formation – central sector), gneisses and migmatites (El Portezuelo Metamorphic-Ígneous Complex - western sector), which presents higher proportions of carbonate and basic rocks in the eastern and southern sectors (Sierra Brava Complex) (Turner, 1960; Willner et al., 1983; Aceñolaza et al., 1988; Jèzek, 1990; Omarini et al., 1999; Aceñolaza and Aceñolaza, 2007). The Sauce Guacho and Santa Rosa plutons were intruded in the schists of the Ancasti Formation, although the SW contact of the Santa Rosa pluton is in contact with the gneisses and migmatites of the El Portezuelo Metamorphic-Igneous Complex (Fig. 1b).

The Ancasti Formation is constituted by banded schists (Qtz-Pl-Bt ± St ± Grt), calc-silicate rocks (Qtz-Act-Czo ± Grt) and quartz micacites (Qtz-Pl-Ms-Bt), with low to medium metamorphic grade (Knüver, 1983; Baldo et al., 2008; Verdechia et al., 2012; Acosta Nagle et al., 2017). These units grade transitionally to gneisses and migmatites of the El Portezuelo Metamorphic-Igneous Complex (Qtz + Kfs + Bt; Crd + Grt + KFelds + Sill) (mineral abbreviations according to Whitney and y Evans, 2010) (Fig. 1b). Based on regional correlations and rock compositions, their protoliths are considered equivalents of the later Proterozoic – early Cambrian Puncoviscana Formation (Rapela, 1976; Rossi de Toselli et al., 1976; Toselli et al., 1978; Aceñolaza et al., 1990; Becchio et al., 1999; Büttner et al., 2005; Durand, 1996; Rapela et al., 1998; Murra et al., 2011). The main migmatization event has been dated between 477 and 470 Ma and the metamorphic conditions have been estimated around 670–820 °C and 4.5–5.3 kbar (Larrovere et al., 2011; Rapela et al., 2007; Murra et al., 2011). On the other hand, the Sierra Brava Complex is composed by meta-carbonate rocks (Cal + Ms + Phl + Qtz ± Gr), meta-psammites (Ms + Bt + Chl + Grt), meta-basic schists (Am + Ep + Chl + Pl) and gneisses and migmatites in the eastern and southern sectors of the mountain range (Miller and Willner, 1981; Aceñolaza et al., 1981; Willner et al., 1983; Knüver, 1983; Baldo et al., 2008; Murra et al., 2011). Towards the northeast, the contact between the Sierra Brava Complex and the Ancasti Formation is constituted by El Alto shear zone (Acosta-Nagle et al., 2024) (Fig. 1b). The protoliths of the Sierra Brava complex have a depositional age between 570 and 590 Ma. (Murra et al., 2011), which relate to the Western Sierras Pampeanas and the Sierra de Tandilia (Rapela et al., 2007; Murra et al., 2011).

## 3. Early Carboniferous Santa Rosa and Sauce Guacho plutons: field relationship, internal structures, and petrographic features

The Santa Rosa and Sauce Guacho plutons are zoned, syeno-monzogranitic, strongly peraluminous, magnesian and high-K plutons. They present ℇNd(t) values of −5.3 (Sauce Guacho) and −5.7 (Santa Rosa), typical of crustal sources without substantial mantle contribution (Toselli et al., 2011).

The igneous bodies present elongate (Santa Rosa pluton) and

ellipsoidal (Sauce Guacho pluton) external shapes, with the greater elongation in NE-SW direction, showing mostly discordant and sharp contacts with the main structure of the Ancasti Formation (Fig. 3a), roughly striking N-S (Fig. 1b). Both granitic bodies are constituted by two main magmatic units that present sharp contacts between them (Fig. 2). A Bt-Ms porphyritic, syeno-monzogranite unit (Porphyritic Unit, later PU) presents K-feldspar megacrysts of 6–9 cm of size, varying from 15 to 25 vol%. Megacrysts are included in a coarse-to medium-grained matrix composed of quartz, alkaline feldspar, plagioclase, biotite, and muscovite, with ilmenite, apatite, monazite, and zircon as main accessory phases. The preferred orientation of K-feldspar megacrysts defines an internal magmatic fabric parallel to the contacts between igneous units (Fig. 2). A second granitic unit is an equigranular, Ms syeno-monzogranite (Equigranular Unit, later EU), with a medium to coarse grain size and compositionally more evolved than the PU and composed of quartz, microcline, plagioclase, muscovite, apatite and zircon. Scarce metasedimentary xenoliths are observed along the contacts with the host rocks.

The Santa Rosa pluton presents an elongate shape with the EU located in its center forming a contorted body with a main axis in a NW-SE azimuth. This unit presents central porphyritic facies with large quartz crystals, alkaline feldspar, and clusters of opaque crystals into an aplitic matrix composed of quartz, microcline, plagioclase, and muscovite. The preferred orientation of K-feldspar megacrysts in the external PU defines a magmatic foliation with ENE-WSW strike at the NE and SW

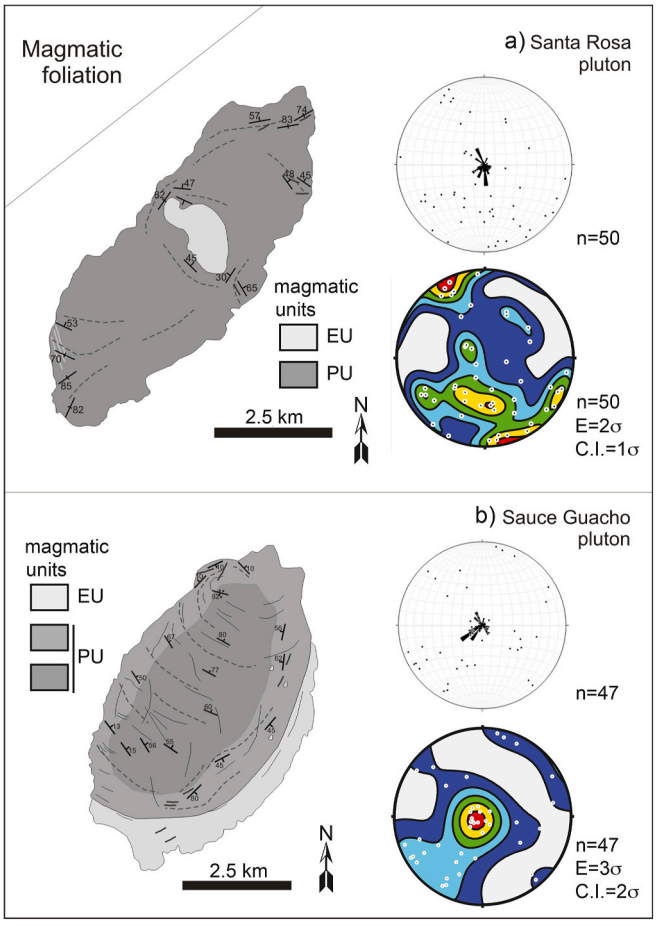


**Fig. 2.** Magmatic foliation maps within the Santa Rosa and Sauce Guacho plutons. Equal area, lower-hemisphere projections and rose diagrams of magmatic foliation. Contours according to the Kamb (1959) method (here and in the rest of this work). Magmatic units (EU and PU) explained in the main text. Spherical projections throughout this manuscript: Stereonet program (Allmendinger et al., 2012; Cardozo and Allmendinger, 2013).

ends of the intrusive body, oblique to the contacts with the metasedimentary host and dipping with high-angle to the NNW and SSE (Fig. 2a). In the central sector, the foliation becomes parallel to the internal contact with the (inner) Ms syeno-monzogranite unit, where it mostly presents inward, medium-angle dips (Fig. 2a). The Sauce Guacho pluton presents an inverse, concentric, compositional zoning, with an asymmetric pattern around a center located in the NE sector of the pluton (eccentric pattern). The inner domain (PU) is constituted by a biotite-rich, porphyritic facies, and the EU is located in the eastern and southern edge of the body, embracing the PU (Fig. 2b). The magmatic foliation presents an ellipsoidal trajectory to the south of the pluton. It mimics both the external shape of the pluton and the internal contact between the granitic units in the eastern side (Fig. 2b). The magmatic foliation ($S_m$) is generally concordant with the contact with the host rocks. The foliation traces describe a concentric pattern in the NE part of the body. Medium-angle, inward dips of $S_m$ dominate the central and the SW sector of the pluton. In the contact zone with the EU, the magmatic foliation presents an NE-SW direction and moderate dips toward the west. This foliation pattern transitions towards the S of the intrusive body into an elongate NE-SW domain with foliations dipping towards the SE. (Fig. 2b).

Both plutons present syn- and post-magmatic aplo-pegmatitic dykes sub-parallel to the magmatic foliations. The syn-magmatic dykes present magma-magma contacts with lobulated shape (Fig. 3b). On the contrary, the post-magmatic dykes present sharp contacts and a tabular shape (Fig. 3c and d). Besides, miarolitic cavities with quartz and feldspar (Fig. 3e), chalcedony-quartz veins with banded structure associated with fluorite veins are present. Particularly, the Sauce Guacho pluton shows a set of pipes located in the NE sector of the body, where the major axis of microcline megacrystals are parallel to the dyke's wall (Fig. 3f). Equigranular granitic xenoliths are present near the contact between the igneous units which may be interpreted as autoliths (e.g., Rodríguez and Castro, 2017; 2018; Fernández and Castro, 2018) (Fig. 3g). Annular fractures parallel to magmatic foliation were also observed in the Sauce Guacho pluton (Fig. 3h). The post-magmatic dykes are parallel to these fractures.

## 4. Structural characteristics of the host rock

In the studied area, the Ordovician main tectonic fabric of the metamorphic rocks ($S_2$ foliation) of the Ancasti Formation presents a regional NNW-SSE strike dipping to the WSW (Fig. 4, $S_2$ external), with average orientation 166°/67°SW, while around the Santa Rosa pluton the S2 foliation dip to the E (Fig. 4). It is associated with the transposition of previous structures and fabrics by isoclinal folding, with main horizontal coaxial shortening around the E-W direction (Miller et al., 1978; Willner, 1983). A relic foliation ($S_1$), oblique to the main structure, is present like inclusion trails in biotitic porphyroblasts of this metasedimentary sequence (Willner, 1983; Baldo et al., 2008; Acosta Nagle et al., 2017). Also, brittle-ductile shear zones, parallel to the main structure and located in the contact with the Sierra Brava Complex (Fig. 4), are linked with retrograde metamorphism and cataclasis associated with a gradual exhumation of the metamorphic domain (Willner, 1983; Acosta Nagle et al., 2017; Acosta-Nagle et al., 2024).

Around the Santa Rosa and Sauce Guacho plutons, the main penetrative structure of the Ancasti Formation ($S_2$) presents a slight but significant variation in its orientation. Around the Santa Rosa pluton, it still shows a NNW-SSE azimuth and medium to high dips toward the E, (Fig. 4). Around the Sauce Guacho pluton, $S_2$ only deviates slightly from the regional trend, although it rotates close to the pluton from the external NNW-SSE azimuth towards N-S or even NNE-SSW strikes and relatively shallower dips (Fig. 4).

Brittle structures crosscut the main fabric of the metamorphic rocks hosting the Santa Rosa and Sauce Guacho plutons. These correspond to kilometer-scale NE-SW faults evidenced by scarps and fault gouge and breccias (Figs. 1 and 4) (Willner et al., 1983). To the NW limit of the

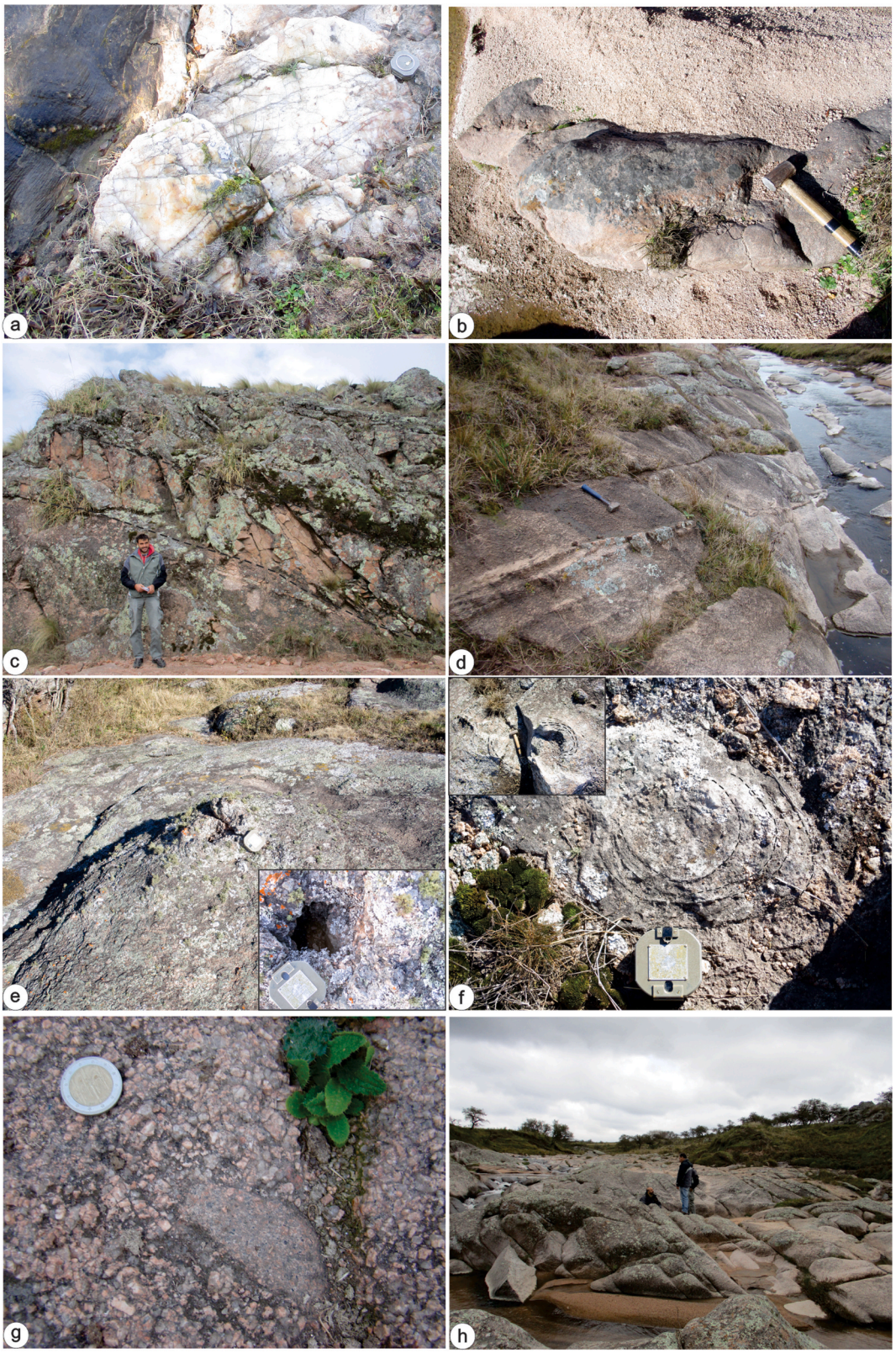


**Fig. 3.** a) Relationship between the metamorphic rock host and plutons (a) and internal structures of the igneous bodies: b) and c) syn-magmatic dykes, d) Post-magmatic dykes parallel to the magmatic foliation and to the fractures, e) Myarolitic cavities, f) Pipes in the NE sector of the pluton, g) Equigranular granite xenolith. h) Diaclases parallel to the magmatic foliation.

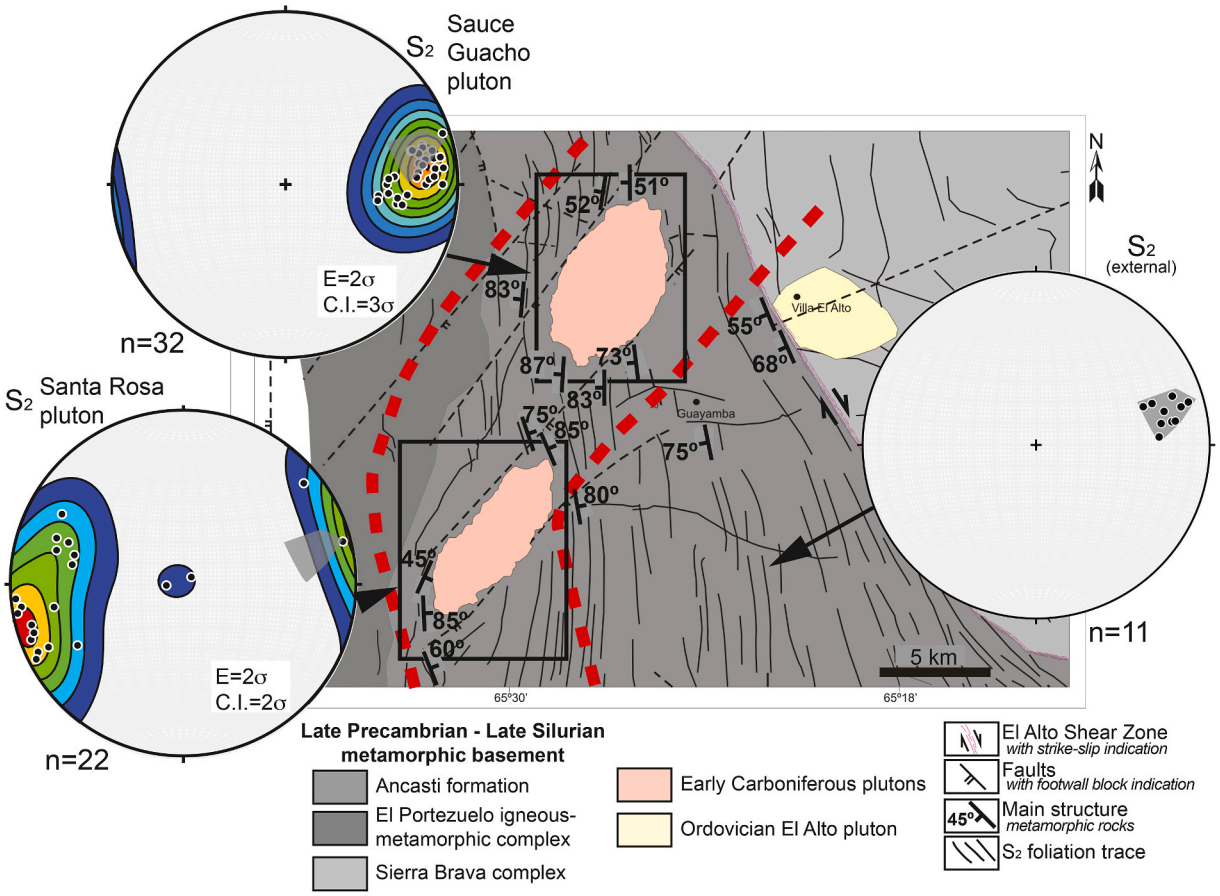


**Fig. 4.** Geological and structural sketch of area of the Santa Rosa and Sauce Guacho plutons. Equal area, lower-hemisphere projections of the regional $S_2$ foliation far (external) and around the Sauce Guacho and Santa Rosa plutons.

range, the normal Alijilán fault was mentioned by Baldis et al. (1975) and Aceñolaza and Toselli (1977) as an important Paleozoic megafracture. Bordering both plutons by the southeast, the normal Mina Dal fault (MD fault in Fig. 1b), with subvertical dip (Ibañez, 1978; Aceñolaza et al., 1983), and the high-angle reverse Santa Rosa fault (SR fault in Fig. 1b) are present (Aceñolaza et al., 1983). Both are associated with mineralized fluorite veins of possible Permo-Triassic age (Ibañez, 1978; Aceñolaza et al., 1983; Zappettini, 1999; Sardi et al., 2023). At the same time, this set of brittle structures with a NE-SW orientation spatially coincides with the northern segment of the trace of the Catamarca Lineament (Baldis et al., 1975), a regional structure that limits the north of the Sierra de Ancasti, south of the Ambato block and east and south of the Sierra de Velasco (Figs. 1 and 4). This lineament corresponds to a structural anisotropy inherited from a long and complex geological history.

## 5. Gravity, density and magnetic susceptibility features

Gravity was used to determine the geology at depth and, together with the density data, to obtain the geometry of the pluton in 3D and locate the possible feeder channels or other structures associated with the ascent and emplacement of the magma. Furthermore, magnetic susceptibility data were used as a reference for the petrophysical parameters and compositional differences within the pluton and host rock.

### 5.1. Methodology

Gravity data at 126 stations were acquired with a Scintrex CG-3 gravimeter and heights were referenced to the ellipsoidal of the WGS84 using a Trimble 5700 Differential GPS. The spacing between each station was 250 m within the intrusive body and near the contacts, and 500 m–1000 m in the most distant sectors. Gravity data were referred to the IGSN71 network. Density values were determined in the laboratory from igneous and metamorphic rocks samples (36 samples, Table 1), according to the method of double weighing with paraffin (Smithson, 1971; Christiansen et al., 2019). The magnetic susceptibility of the different units (Table 1) was measured on-site with an SM-30 of Terraplus USA Inc. Magnetic susceptibility meter, averaging at least three and five measurements within a radius of 50 m in every station.

The physical attributes of density and magnetic susceptibility were used only as reference input for the petrophysical parameters of the lithological units, and their differences may be due to compositional and mechanical variations. In the case of magnetic susceptibility, there is a possible range of values of two to four orders of magnitude for any lithological group (Clark, 1997), in addition to the fact that rock weathering can decrease magnetic susceptibility values due to the nature of metastable minerals such as magnetite and pyrrhotite on the Earth's surface (Isles and Rankin, 2013).

Gravity data were processed through the Oasis Montaj program to do the free air (CAL), Bouguer (CB), and topographic (CT) corrections and obtain the Complete Bouguer anomaly map using a reference density of 2670 kg $m^{-3}$ (LaFehr, 1991; Hinze, 2003; Hinze et al., 2005). The high-frequency noise in the Bouguer anomaly grid was removed by a 9 x 9 convolution filter. Furthermore, anomalies were separated into regional and residual contributions using an upward continuation filter.

Inversion and modeling of the data were carried out using Geomodeller software (Calcagno et al., 2008; Guillen et al., 2008). The method was developed for scenarios where geological knowledge is sporadically available across the surface area. Drawing upon the principles of potential field theory, this approach both interpolates and

**Table 1**
Lithology type, density and magnetic susceptibility data.

| Station | Latitude/Longitude | | Lithology type | Density | | Magnetic Susceptibility | |
|---|---|---|---|---|---|---|---|
| | | | | Nº of samples | Density (kg m$^{-3}$) | Nº of measurements | Average (SI) |
| A033 | −28.396222 | −65.487068 | Porphiritic granite (Santa Rosa) | 4 | 2480 ± 37.6 | 5 | 0.000191 ± 0.000116 |
| A037 | −28.395827 | −65.498068 | Equigranular granite (Santa Rosa) | 4 | 2540 ± 15.0 | 4 | 0.00003275 ± 0.000011 |
| A072 | −28.300743 | −65.425412 | Equigranular granite (Sauce Guacho) | 4 | 2470 ± 22.5 | 3 | 0.000009 ± 0.000003 |
| A075 | −28.296856 | −65.432184 | Porphiritic granite (Sauce Guacho) | 4 | 2470 ± 20.9 | 5 | 0.0000798 ± 0.000014 |
| A014 | −28.365241 | −65.415738 | Schist (regional) | 4 | 2680 ± 11.4 | 5 | 0.000313 ± 0.000063 |
| A021 | −28.388804 | −65.448360 | Schist (regional) | 4 | 2690 ± 15.7 | 3 | 0.000188 ± 0.000031 |
| A123 | −28.344355 | −65.442472 | Schist (near the pluton) | 4 | 2540 ± 19.8 | 4 | 0.0002867 ± 0.000074 |
| A052 | −28.417415 | −65.539639 | Schist (near the pluton) | 4 | 2430 ± 46.4 | 3 | 0.000124 ± 0.000017 |
| A119 | −28.350784 | −65.482163 | Schist (near the pluton) | 4 | 2500 ± 40.7 | 5 | 0.0003264 ± 0.000155 |

extrapolates data, considering the geological contacts, their orientations, and the sequence of formations within the stratigraphic column. The goal is to construct a 3D model that delineates the shape and petrophysical characteristics of the geological units (McInerney et al., 2005). Subsequently, the model is divided into voxels (three-dimensional rectangular prisms characterized by the geological unit they symbolize) to facilitate computational analysis. Through a process of forward modeling, the geological units within the model are refined, aiming to closely match their geophysical signals with those of the original geophysical grids, and are then refined through a least squares analysis, leading to further adjustments in the model. Ultimately, a litho-constrained stochastic inversion process is implemented (following Christiansen et al., 2019). As a result, we obtain the geometry of the pluton constrained by petrophysical, geophysical and geological data.

### 5.2. Results

The residual Bouguer anomaly map (Fig. 5a) shows a gravimetric low (−47.39 mGal) with an elongated shape in NE-SW direction and arcuate in its SW extreme, of 7.5 km wide. Within this area, two other local gravimetric lows are observed (between −52.15 and −49.64 mGal), one with an elliptical shape, corresponding to the Sauce Guacho pluton, and another less defined corresponding to the Santa Rosa pluton. The location and orientation of the elongated gravimetric low coincide both with the alignment direction of igneous bodies and with the location and orientation of the set of brittle structures (Mina Dal and Santa Rosa faults). Besides, differences in density values of approximately 100 kg m$^{-3}$ between the Ancasti Formation around the plutonic bodies (2610 kg m$^{-3}$) and the most distant sectors (2710 kg m$^{-3}$) would be linked to the presence of these brittle structures, and the deflections linked to expansion of the plutons, since no lithological changes in surface were observed. The Santa Rosa and Sauce Guacho plutons present density values between 2530 and 2470 kg m$^{-3}$ (Table 1) and coincide with the lowest gravity values. These differences in density values allowed the development of a gravimetric inversion model for the Sauce Guacho pluton and its environment (Fig. 5). The Sauce Guacho pluton resulted in a density of 2470 kg m$^{-3}$ (Fig. 5b), the metamorphic host rock near to the pluton resulted in a density of 2610 kg m$^{-3}$ (Fig. 5c) and the metamorphic host rock further from the pluton resulted in 2710 kg m$^{-3}$ (Fig. 5d). The profiles corresponding to the major (Fig. 5e) and minor axes (Fig. 5f) of the body show an area with greater thickness in the NE sector of the body, which gradually decreases towards the SW. In the thickest area, up to three elongate bands, sub-perpendicular to the major axis of the body, and with cylindrical or tubular geometry, affecting the bottom of the pluton, are distinguished. These bands could be interpreted as feeder channels or as due to corrugation or folding of the contact between the pluton and its host rock.

In the Santa Rosa pluton case, with a density of 2530 kg m$^{-3}$ (Table 1), the lack of data in the western and southern sectors of the study area does not allow the construction of a gravimetric inversion model for the pluton. However, this zone constitutes the contact between the granitic pluton, and the gneissic and migmatite rocks of the El Portezuelo Metamorphic-Igneous Complex, where a lower-density contrast is expected.

The magnetic susceptibility values between 1,0 x10 $^{-5}$ SI and 3,1 x 10$^{-4}$ SI for the Santa Rosa and Sauce Guacho plutons show a paramagnetic granite with ilmenite tendency, typical of granitic magmas formed into the upper-middle crust (Ishihara, 1977; Clark, 1999). Particularly, the PU unit of the Santa Rosa plutons presents slightly higher magnetic susceptibility values than the EU unit. In the Sauce Guacho case, differences between its units were not observed (Table 1).

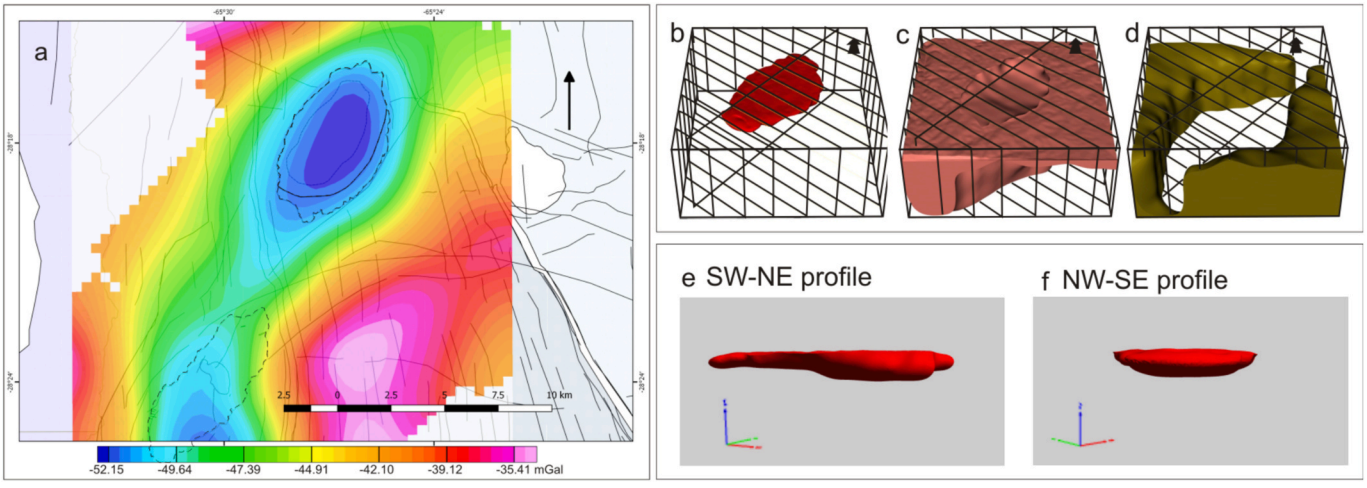


**Fig. 5.** Gravity data. a) Bouguer anomaly map, NW of Sierra de Ancasti. b) Inversion model of Sauce Guacho pluton: c) Geometry of the lower boundary of the pluton. d) Metamorphic host rock close to the pluton. d) and e) SW-NE (longitudinal) and NW-SE (transversal) profiles of the pluton.

## 6. Kinematic analysis

The geometric and structural characteristics of the plutons and their country rock and the observation of an arcuate gravity anomaly interpreted as a deformation zone that includes both plutons suggest a possible structural control during the emplacement of the igneous bodies. Due to the little structural evidence at the outcrop level to establish the tectonic control in the emplacement of the plutons by the pre-existing structure, a more rigorous evaluation involves a detailed kinematic study using all available tectonic and magmatic structures and fabrics previously described in this work.

### 6.1. Methodology

Given the structural and gravimetry data about the elongated deformation zone and the absence of more detailed information in the study area about this structure, we have chosen to assume a simple analytical model of monoclinic transpression/transtension shear zone (e.g., Passchier, 1998), with the simple shear (non-coaxial) component acting parallel to the strike of the shear zone, and the direction of maximum stretching (transpression) or shortening (transtension), associated with the pure shear component (coaxial component), located according to the dip direction of the shear plane. The parameters controlling the kinematic model are (see e.g., Fernández and Díaz Azpíroz, 2009, 2022, for further explanations of those parameters): $\phi$, the pitch of the simple shear direction on the shear plane; $\iota$ or $\upsilon$, the angle between the shortening –transtension- or stretching –transpression- direction of the pure shear component and the dip direction of the shear plane, respectively; $k$, value of the Flinn shape parameter corresponding to the coaxial component for pure shear; $W_k$, kinematic vorticity number (Truesdell, 1953). The following values of the involved parameters have been chosen: $\phi = 0°$; $\iota$ or $\upsilon = 0°$; $k = 1$; $W_k$: Values were explored assuming the predominance of the coaxial component (0.2, 0.4, 0.6), the non-coaxial component (0.9, 0.99, 0.9999) and for the boundary between both (0.81).

The orientation of the boundaries of the shear zone is a fundamental element in this case, given that, in the studied area, there are few structural elements at the emplacement level. Accordingly, up to five different conceptual models have been considered to simulate the shear zone influence on plutons emplacement (Fig. 6). Conceptual models 1 to 4 consider a curved shear zone, following the geometry of the gravity anomaly identified in this work (Fig. 5). In all these cases, the northern segment of the curved shear zone, around the Sauce Guacho pluton, would be oriented 040°/90°, following the trend of the gravity anomaly and considered as the large-scale attitude of the Catamarca Lineament. More difficult is to ascertain the orientation of the southern segment of the curved shear zone, around the Santa Rosa pluton. Several possibilities were tested, all of them following an NNW-SSE strike, which is the trend of the gravity anomaly in the southern area. After discarding the geometries that do not allow an adequate explanation of the available data, it was decided to simulate the orientation of the shear zone in its southern segment using the average strike and dip of the main anisotropy ($S_2$) of the country rocks, that is: 166°/67°SW. More detailed arguments for this choice will be given later. The conceptual model 5 simulates a shear zone parallel to the supposed regional layout of the Catamarca Lineament, both for the Sauce Guacho pluton and the Santa Rosa pluton, that is: 040°/90°.

Due to the scarce reliable kinematic criteria about the movement sense of the deformation zone, all the possibilities were considered (Fig. 6). Thus, conceptual models 1 and 3 propose a dextral displacement for the shear zone, which shows two possibilities due to its curvature. In model 1, the southern segment mainly accommodates a simple shear component, forcing the northern segment to show transtensional kinematics. In model 3, simple shear predominates in the northern segment, forcing a transpressional setting in the southern segment. In contrast, conceptual models 2, 4, and 5 propose a sinistral displacement for the shear zone. Model 5 assumes a planar shear zone, while the curvature implied in models 2 and 4 leads to a variation in the kinematics of the northern and southern segments. Simple shear predominates in the southern (model 2) or northern (model 4) segments, leading respectively to transpression in the northern segment (model 2) and transtension in the southern segment (model 4).

The analytical kinematic model used in this work (e.g., Fossen and Tikoff, 1998; Fernández and Díaz Azpíroz, 2009) allows determining, for

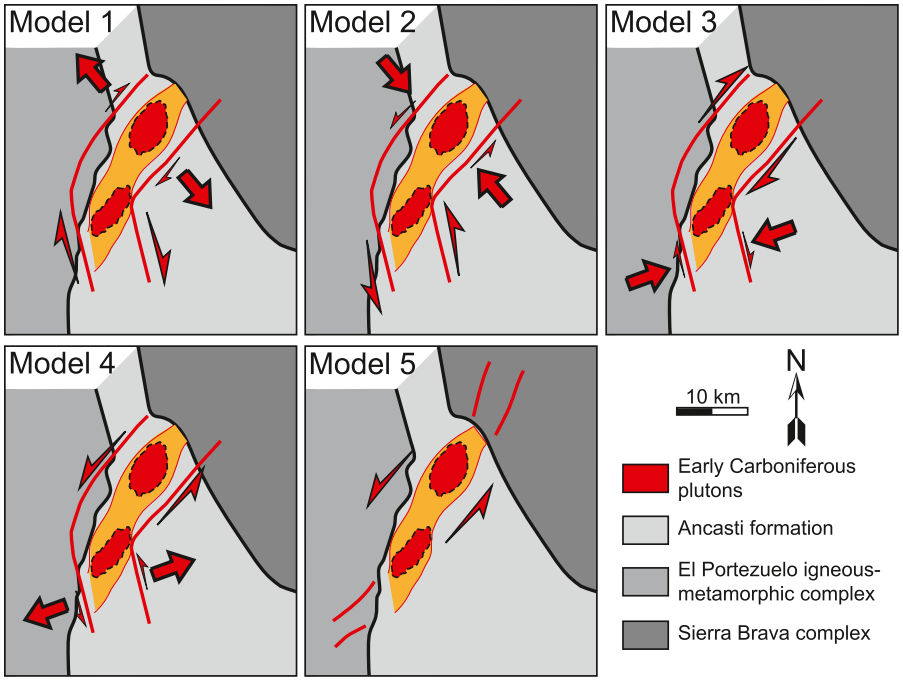


**Fig. 6.** Distinct conceptual models that can be proposed to account for the emplacement of the Sauce Guacho and the Santa Rosa plutons within a shear zone.

each conceptual model and combination of parameters: the orientation of the main axes of the infinitesimal and finite strain ellipsoid ($X$, $Y$, $Z$); for the southern segment of the curved shear zone in models 1 to 4 (non-vertical shear zone), the orientation of the long and short axes of the strain ellipse in a horizontal plane; and the reorientation that the $S_2$ planes (or their poles) undergo inside the shear zone as the magnitude of the finite deformation increases. The results and predictions of the analytical kinematic model for each conceptual model are compared with the orientation of $S_2$ in the vicinity of both plutons as a criterion to check the conceptual models that are kinematically compatible with the observed structures and to constrain the possible range of vorticity values involved in the process of pluton emplacement. Additionally, the horizontal outline (Sauce Guacho and Santa Rosa plutons) or 3D shape (Sauce Guacho pluton) of the intrusive bodies, as well as the geometric pattern of the magmatic foliation ($S_m$) in each pluton, are evaluated in the light of the kinematic model to better understand the kinematics of the shear zone.

### 6.2. Results

The results of the analytical model simulating the conceptual models considering a sinistral simple shear component (models 2, 4, and 5) fail to reproduce the natural structures and fabrics. In particular, the reorientation trajectories of the $S_2$ poles (red arrows in Fig. 7) predicted by the analytical model for conceptual models 2, 4, and 5 are very different from those observed close to the Sauce Guacho pluton. Regarding the Santa Rosa pluton, the trajectories predicted for conceptual models 2 and 4 are more similar to the natural ones, although the modeled and observed $S_2$ poles do not coincide in the case of conceptual model 5. The axis of maximum infinitesimal shortening in the horizontal predicted by the analytical model varies in orientation between NNE-SSW and NW-SE (Fig. 7). These orientations would be congruent with the strike of the supposed feeder channels suggested by the geophysical and geological information (Fig. 5c). These structures should have rotated counterclockwise toward perpendicularity with the boundary of the shear zone with the increase of the finite deformation (e.g., Fernández and Díaz Azpíroz, 2022). However, for any of these conceptual models to be considered viable from a kinematic point of view, it would be necessary for both plutons to simultaneously show an acceptable match between the predictions of the analytical model and natural observations. It can be seen in Fig. 7 that this fit is not possible for conceptual models 2 and 4, which present a reasonable match between the analytical model and reality for the Santa Rosa pluton but not for the Sauce Guacho pluton. As for conceptual model 5, it does not show compatibility for any of the plutons.

The predicted reorientation for the $S_2$ poles under conceptual model 3 is fairly consistent with the natural data for the Sauce Guacho pluton, but not for the Santa Rosa pluton (Fig. 8). Conceptual model 1 shows the best fit for both plutons. Specifically, the reorientation of the $S_2$ poles predicted by the analytical model fully covers the dispersion of these poles observed around the Sauce Guacho pluton (Fig. 8). A reasonable fit is also observed for the Santa Rosa pluton.

## 7. Discussion

### 7.1. Ascent and emplacement associated with a brittle-ductile deformation structure

The Santa Rosa and Sauce Guacho plutons present sharp and discordant contacts with their host rocks. Emplacement-related fabrics

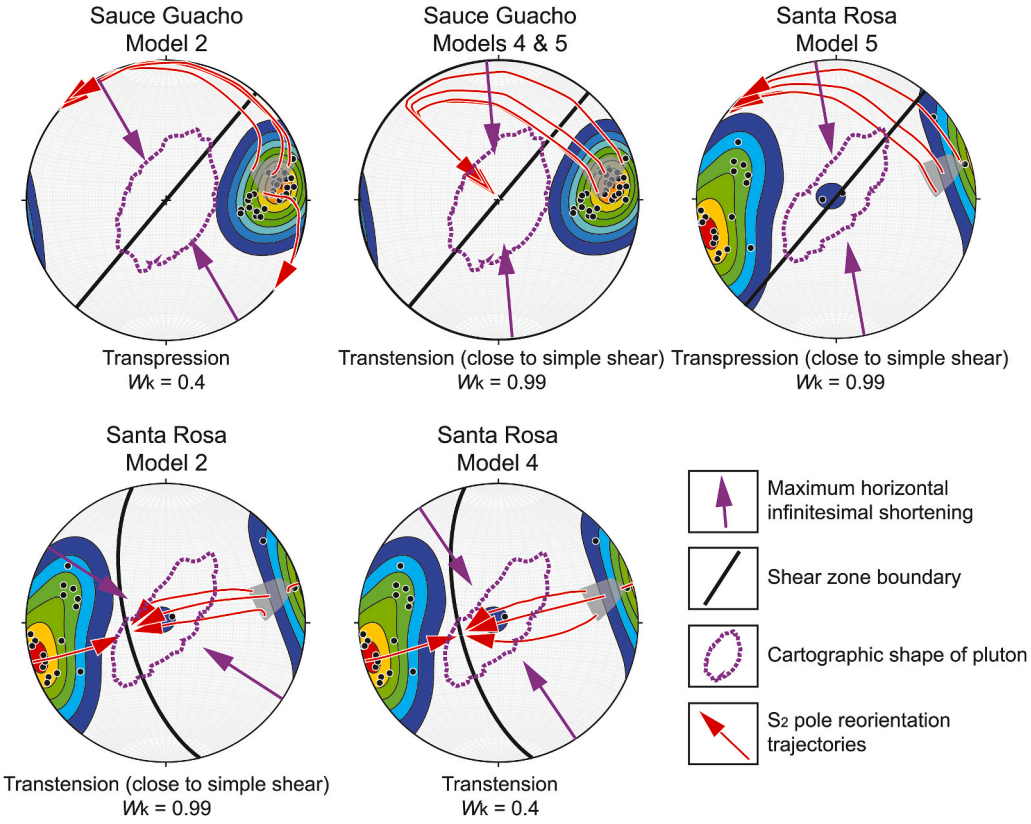


**Fig. 7.** Results of the analytical kinematic model of transtension/transpression applied to conceptual models 2, 4, and 5. Equal area, lower-hemisphere projections illustrate the orientation of $S_2$ measured around both plutons (density plots and black dots), as well as the predictions of the kinematic model (red arrows). The external outline (purple dashed lines) of the plutons is also represented on the plots, together with the trend of the maximum horizontal infinitesimal shortening (purple arrows) according to the kinematic model. $W_k$ is the kinematic vorticity number. (For interpretation of the references to colour in this figure legend, the reader is referred to the Web version of this article.)

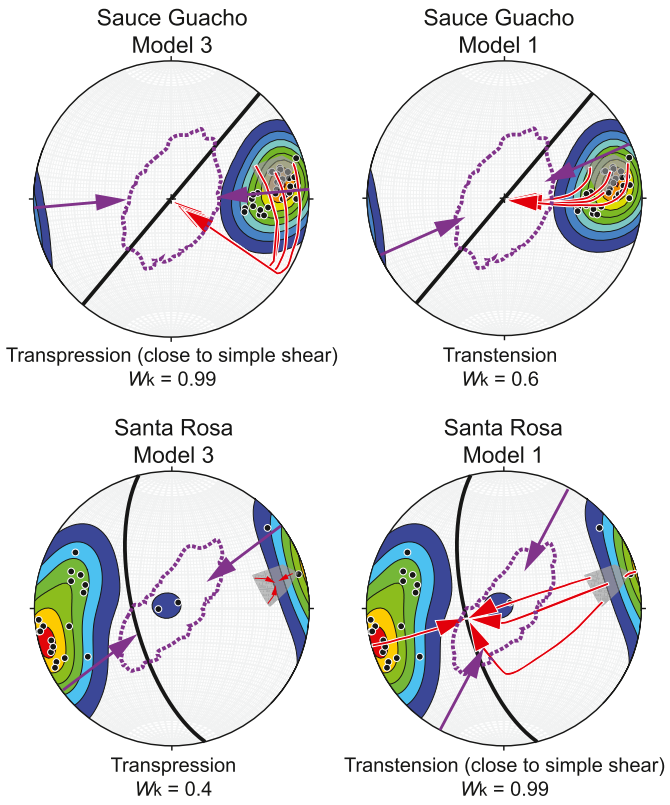


**Fig. 8.** Same as Fig. 7, but for conceptual models 1 and 3.

are post-kinematic relative to the main ductile structures of metamorphic rocks ($S_2$ foliation). These characteristics, and the presence of syn- and post-magmatic dykes, suggest an emplacement in the brittle shallow crust, with a high rheological contrast between intrusive magma and host rock (Daly, 1933; Campbell and Turner, 1989; Castro Dorado, 1989; Valentine, 1992; Pinotti et al., 2002; Žák et al., 2006; Llambias, 2008). In this emplacement level, the flow of granitic magma batches would be channelized through brittle-ductile structures (Vigneresse, 1995; Clemens, 1998; Tobish and Paterson, 1990; Hutton and Reavy, 1992; Guillet et al., 1985; Hutton and Reavy, 1992; Clemens and Mawer, 1992; Petford et al., 2000; Aragón et al., 2019). Fabrics and structures within both studied plutons are mostly sub-parallel to their external contacts, suggesting that they were formed during the emplacement (Hutton, 1988; Fernández and Castro, 1999). The geophysical and structural evidence presented and discussed in this work points to a tectonic control in the emplacement and, probably, also in the ascent of magmas that gave place to Santa Rosa and Sauce Guacho plutons. Alternatively, the assumed structural control may simply be conditioned by the injection of magma and the consequent modification of the stress field in the host rocks. If we choose the intermediate alternative, that is, that there is positive feedback between magmatic and tectonic stresses (e.g., Hutton, 1997; de Saint Blanquat et al., 1998; Brown and Solar, 1998), and assuming that the available magmatic structures and fabrics are very scarce, we will next evaluate the role of regional structures in the study area during the emplacement process of both intrusive bodies, which ultimately also respond to the influence of the emplacement of magma batches. An arcuate, NE-SW-trending low gravity anomaly, 5.7 km wide, coincide with the ubication and orientation of the set of the brittle structures and is aligned with the major axes of the intrusive bodies, which it includes (Fig. 5). The low gravity anomaly that corresponds to the granites shows that could continue in depth. Since no lithological variations within the host rocks or contact metamorphic aureoles were observed on the surface, this low gravity in cone shape is interpreted as variations in the mechanical behavior of host rocks, whose evidence is the presence of weakness zones in the crustal rocks. The structural control of pluton emplacement proposed in this work expresses a very specific interaction between a larger structure (shear zone) and the extension fractures associated with its kinematics, in line with previous works that illustrate the emplacement of plutons in extensional and contractional settings (Hutton, 1982, 1988; Brun and Pons, 1981; Courrioux, 1982; Murphy, 1987; Hutton and Reavy, 1992; Fernández and Castro, 1999; Aranguren et al., 1997; D'Eramo et al., 2006; Stevenson et al., 2008). The main brittle-ductile deformation structure to which the emplacement of the granitic plutons seems related, shows little surface evidence, which may be due to an emplacement in shallow crustal levels (D'Eramo et al., 2006, 2013; Aranguren et al., 1997). Indeed, in many cases the presence of extensional structures associated with concealed shear systems are inferred by the shape in the map of igneous bodies, their fabric orientation, and by gravimetric data (Castro, 1986; D'Eramo et al., 2006; Fernández and Díaz-Azpíroz, 2022).

### 7.2. *Structural control and emplacement mechanisms of the Sauce Guacho and Santa Rosa plutons: kinematic evaluation*

Among the most important and striking facts of the structure associated with the emplacement of the Sauce Guacho and Santa Rosa plutons, two can be highlighted: the distinct configuration shown by the reoriented regional foliation ($S_2$) around both plutons (Fig. 4), which could also respond to the pluton's expansion, and the differences in their external shapes and the pattern of magmatic foliation ($S_m$; Fig. 2). As a result, the shear zone responsible for the emplacement of both plutons must vary in orientation, kinematics, or both from one pluton to another. The results of the analytical kinematic model indicate that a shear zone with the same orientation and kinematics for both plutons (e.g., conceptual model 5) is kinematically infeasible (Fig. 7). Therefore, it is necessary to consider segments with different orientations of the shear zone, which is also based on the pattern of gravity anomalies identified in this work (Fig. 5). In this sense, the curvature of the shear zone inevitably imposes different vorticities for the two segments considered (the north, where the Sauce Guacho pluton is included, and the south, with the Santa Rosa pluton). As for the simple shear component, it can be considered dextral or sinistral. Again, the analytical model of $S_2$ reorientation appears to exclude sinistral displacements (Fig. 7). The results of the analytical model coincide with the qualitative observation of the clockwise reorientation of the $S_2$ traces around the Santa Rosa pluton. Although less marked, this same type of reorientation of $S_2$ can also be seen in the vicinity of the Sauce Guacho pluton. Of the two possible conceptual models considering a dextral curved shear zone, the one in which the southern segment (Santa Rosa) would show kinematics close to simple shear, while in the northern segment (Sauce Guacho) transtension would predominate (conceptual model 1), seems the most valid from a kinematic point of view (Fig. 8). Conceptual model 1 will be taken as a basis to analyze how the rest of the structural features within and in the vicinity of both plutons could be explained.

Concerning the Sauce Guacho pluton, the orientation of the short horizontal axis (*Y*, in this case) of the finite strain ellipsoid predicted for conceptual model 1, for vorticity values with a predominance of pure shear ($W_k$ = 0.1 to 0.6), coincides with the arrangement of the largest diameter of the pluton (Fig. 9). This parallelism is less marked with increasing vorticity and the magnitude of the finite deformation. The geometry of the open fracture in the host rock around the Sauce Guacho pluton, determined in this work through the gravimetric study (Fig. 5d), is compatible with the average orientation of the maximum horizontal shortening, suggesting that it is an extension fracture (T-fracture). The clockwise rotation of the *Y* axis with increasing deformation also seems to coincide with the slightly sigmoidal geometry of that fracture. At this point, it is worth asking about the meaning of the corrugated structures, elongated in the NW-SE direction, detected in the gravimetric study of pluton (Fig. 5c). These elongated structures could be interpreted as

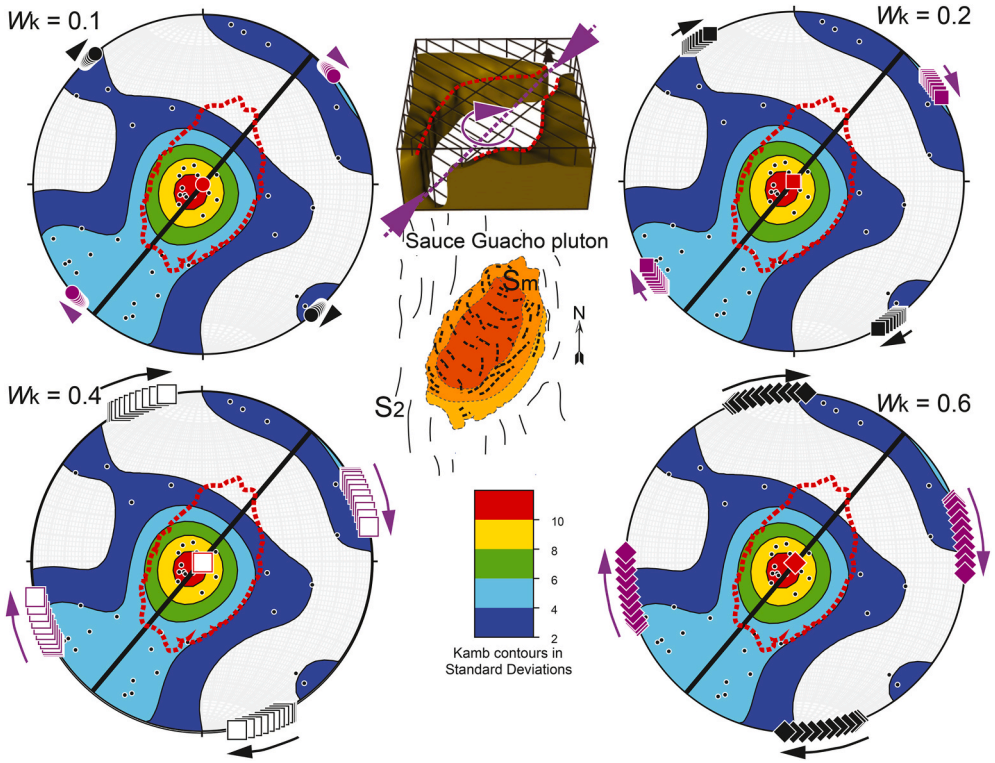


**Fig. 9.** Comparison of the external map outline (red dashed lines), host-rock shape (given by the gravimetric study), and pattern of magmatic foliation ($S_m$, equal area, lower-hemisphere projections, see also Fig. 2) for the Sauce Guacho pluton with the orientation of the principal axes of the infinitesimal and finite strain ellipsoid according to the results of the kinematic model (long axis, *X*: black; intermediate axis, *Y*: purple; short axis, *Z*: red; arrows indicate the rotation of the principal axes with increasing finite deformation magnitude). Conceptual model 1, $W_k$ is the kinematic vorticity number. The trend of the maximum horizontal shortening (in this case, the *Y* principal strain axis) is also shown with purple arrows on the 3D reconstruction of the host-rock shape around the pluton obtained from gravimetry (Fig. 5d). (For interpretation of the references to colour in this figure legend, the reader is referred to the Web version of this article.)

feeder channels or, alternatively, perpendicular structures parallel to the maximum horizontal shortening as suggested Fig. 9. It is possible to evaluate both possibilities kinematically by way of analyzing the initial orientation and the subsequent rotation of the extension fractures in the transtension regime and under different vorticity values (Fernández and Díaz Azpíroz, 2022). The initial strike of these extension fractures (for $W_k$ values of 0.1–0.6) is far from that of the elongated structures (Fig. 10). A very high finite strain would be necessary to ensure that the extension fractures were oriented close to perpendicularity to the boundaries of the shear zone (Fig. 10). On the contrary, the transtensional folding model of Fossen et al. (2013) allows for determining the angle between the long axis of the transtension-related folds and the boundaries of the shear zone. Applied to the case of the shear zone of conceptual model 1 for the Sauce Guacho pluton, it is possible to verify that the predicted initial orientation of the fold axes coincides with that of the corrugations evidenced by gravimetry (Fig. 10). The transtensional folding model allows relatively limited rotations of the fold axes, which should remain relatively fixed with increasing finite deformation for low values of vorticity. It can be concluded, therefore, that the elongated structures found through gravimetric analysis probably correspond to open folds sub-normal to the maximum horizontal shortening, nucleated at the contact between the base of the pluton and its host rock because of the viscosity contrasts between both systems. The emplacement mechanism of the pluton was probably conditioned by the nucleation and growth of a large extensional fracture parallel to the average strike of the *Y* axis of the strain ellipsoid. The extensional fracture would have contained the *Y* and *Z* axis of the ellipsoid, both implying shortening under transtension. Regarding the magmatic foliation ($S_m$) pattern in the Sauce Guacho pluton, it is noteworthy that the most important maximum of $S_m$ poles is vertical, parallel to the short axis (*Z*) of the infinitesimal and finite strain ellipsoid (Fig. 9). That is, the vertical shortening led to the formation of sub-horizontal magmatic fabrics. The fact that the best fit between natural data and the transtensional analytical model was accomplished with low vorticities ($W_k \leq 0.6$), in the field of the predominance of the coaxial component, explains the importance of the vertical shortening in the area. This also accounts for the vertically shortened shape of the pluton as deduced from the gravimetric study that shows a tabular shape (Fig. 5). Also remarkable is the presence of a $S_m$ pole girdle sub-parallel to the long axis of the pluton (Figs. 2 and 9), which can be explained as an open, long-wavelength fold resulting from the maximum horizontal shortening (*Y* axis) in the NE-SW direction (Fig. 9). Finally, a girdle of $S_m$ poles in the NW-SE direction is arranged in a direction normal to the long axis of the pluton (sub-parallel to the long axis of the strain ellipsoid, *X*, especially for low vorticity values). It should represent the flow of magma along the fracture walls, parallel to the long axis of the pluton. The elliptic Sauce Guacho pluton presents a slightly eccentric pattern of $S_m$ trajectories in plan view (Figs. 2 and 9), sub-parallel to the contact between the igneous units at the southern and eastern part of the pluton, indicating lateral expansion in a rigid crust (Aragón et al., 2019). The reverse compositional zoning observed in the pluton suggests a low emplacement rate (Vigneresse et al., 1996; Hecht y Vigneresse, 1995; Bachmann and Bergantz, 2004, 2008; Miller et al., 2011), therefore susceptible to being affected by the deformation transmitted by the shear zone (tabular shape, folds in contact with the host rock).

According to the kinematic analysis of conceptual model 1, the Santa Rosa pluton would have been located in a shear zone with a predominance of simple shear ($W_k > 0.81$). The orientation of the *Z* or *Y* axes of the strain ellipsoid or that of the short axis of the horizontal ellipse (which, in this case, does not coincide with the short axis of the 3D ellipsoid since the shear zone is not vertical), is parallel to the longest horizontal diameter of the pluton (Fig. 11). Therefore, it can be

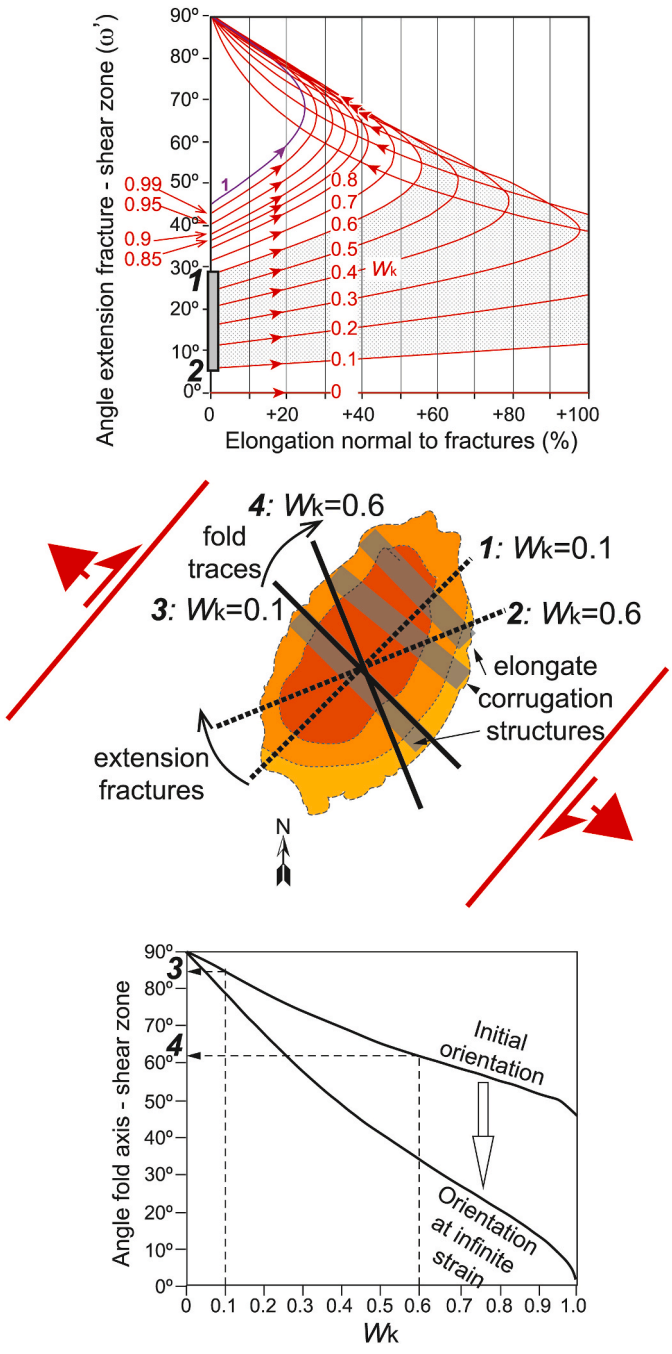


**Fig. 10.** Kinematic evaluation of the formation of elongated structures with an NW-SE trend observed from the gravimetric study on the Sauce Guacho pluton (central sketch). Upper diagram: Initial orientation (gray zone between points 1 and 2) and subsequent rotation of extension fractures for the values of the variables controlling the transtension flow corresponding to the best fit between the kinematic model and natural data (diagram of Fernández and Díaz Azpíroz, 2022). The results are shown as dashed, black lines in the central sketch for the optimal range of vorticity values indicated by the kinematic model ($W_k = 0.1$ to 0.6). Lower diagram: Initial orientation (points 3 and 4) and subsequent rotation of transtension folds for the values of the variables of the kinematic model as explained above (diagram of Fossen et al., 2013). The results are shown as black lines in the central sketch.

suggested that the Santa Rosa pluton follows an emplacement model similar to that of Sauce Guacho, corresponding to an extension fracture, albeit forming here a high angle to the boundaries of the shear zone. The initial angles are between 35° and 45° for $W_k > 0.81$, increasing strongly with the increase in the finite deformation (Fig. 10). The principal maximum of poles of $S_m$ coincides with the *X* axis of the infinitesimal and finite strain ellipsoid, especially for high vorticity values (≥0.99). This fact can be interpreted as a consequence of the magma flow parallel to the NE-SW walls of an extension fracture, roughly coinciding with the pluton that can be seen today. A prominent girdle of $S_m$ poles is observed on the Santa Rosa pluton (Figs. 2 and 11). Geometrically, this girdle indicates that the magmatic foliation defines an arcuate structure whose axis is oriented sub-parallel to the maximum dimension of the pluton (see also the pattern defined by the traces of the $S_m$ visible on the map in Fig. 11), which can be interpreted as the result of magma flow within an elongated dome-shaped plutonic body in a NE-SW direction. Note, however, that the axis of the arched structure described by the $S_m$ is not horizontal, but rather plunges towards the NE and tends to parallelism with the *Z* axis of the strain ellipsoid. The girdle follows the average plane of external foliation ($S_2$) which, in conceptual model 1, defines the orientation of the boundaries of the shear zone (Fig. 11). A weaker $S_m$ pole girdle strikes NE-SW and can be interpreted as representing folds normal to the maximum horizontal shortening, similar to the case of the Sauce Guacho pluton, although much less developed. The $S_m$ trace around the EU unit body, as well as the geometry of this body itself (Figs. 2 and 11), seem to correspond to the interference of both types of folds or arcuate structures. All these observations reveal the importance of structural controls in the magmatic flow in the studied area. The elongated, symmetrical, and normal zoning of the Santa Rosa pluton can be used as evidence of a higher emplacement rate (Vigneresse et al., 1996; Hecht and Vigneresse, 1999; Bachmann and Bergantz, 2004, 2008; Miller et al., 2011). The presence of the regional $S_2$ foliation (NW-SE striking and dipping towards the E) would have been decisive in the case of the Santa Rosa pluton. The $S_2$ planes were penetrative mechanical weakness surfaces that, subjected to the activity of a renewed regional deformation field during the ascent of magma, led to the nucleation along them of a shear zone at the southern segment of the studied region. The shear zone was kinematically close to a simple shearing type of flow. It can be speculated that the deviation of the shear zone's direction towards the SSE in the vicinity of the Santa Rosa pluton is related to the presence to the west of a domain of more resistant or less foliated metamorphic rocks (El Portezuelo Metamorphic-Igneous Complex, Fig. 4), so the shear zone curved towards the SE inside the Ancasti formation.

In summary, it can be concluded that conceptual model 1 allows us to kinematically understand the characteristics of the structures and fabrics within and around the Sauce Guacho and Santa Rosa plutons. The kinematic analysis based on conceptual model 1 and applied to the understanding of the reorientation of regional foliation ($S_2$), and to the evaluation of the external shape and the pattern of magmatic foliation ($S_m$) of each pluton, reveals structural control of the emplacement of both plutons within a transtensional curved shear zone, with a predominance of simple shear ($W_k \gg 0.81$ and probably >0.9) in its southern, NNW-SSW-striking segment (Santa Rosa pluton area), and with a predominance of pure shear ($W_k$ between 0.1 and 0.6) in its northern, NE-SW striking segment (Sauce Guacho pluton area).

### 7.3. Tectonic implications of the NE-SW brittle-ductile shear zone

The Santa Rosa and Sauce Guacho plutons are good examples of granitic bodies emplaced in the shallow crust in an intracontinental setting, as consequence of Carboniferous magmatism at the SW margin of Gondwana (Grosse et al., 2009; Alasino et al., 2012; Toselli and Rossi de Toselli, 2018; Dahlquist et al., 2021; Alasino et al., 2022; Acosta Nagle et al., 2022). From the gravimetric, structural and kinematic study presented in this work, it is possible to shed some light on the tectonic significance of the brittle-ductile shear zone where both plutons were emplaced. A fundamental aspect at this point is to establish the orientation of the relative displacement vector of the blocks separated by this structure. The orientation of the relative displacement vector (divergence angle in the case of transtension) can be determined from the

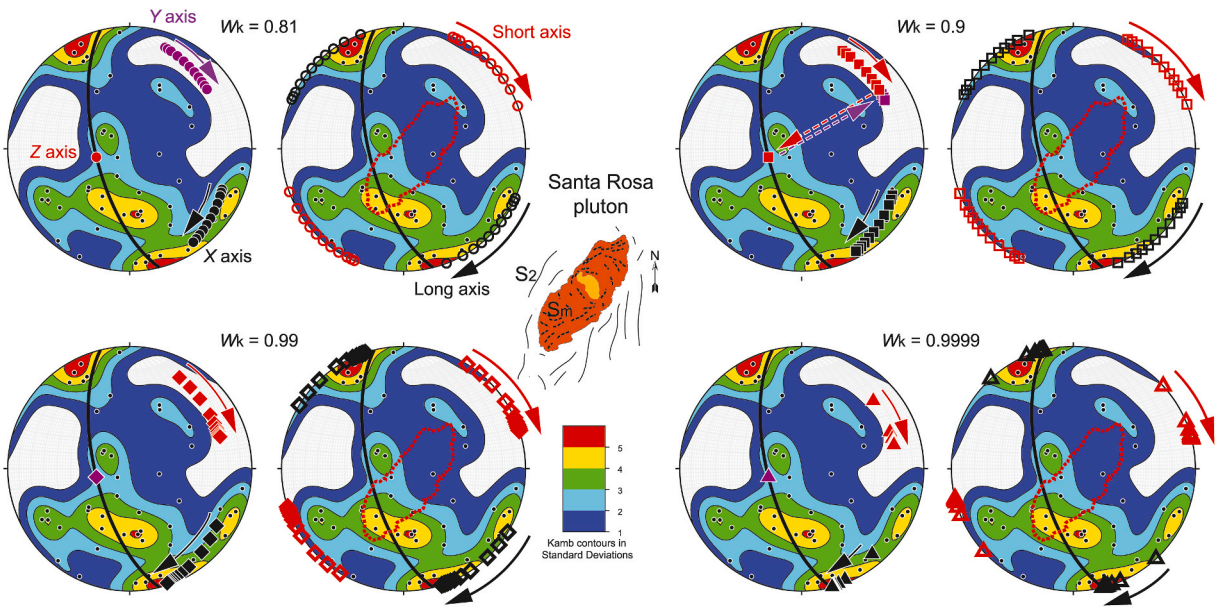


**Fig. 11.** Comparison of the pattern of magmatic foliation ($S_m$, equal area, lower-hemisphere projections, see also Fig. 2) for the Santa Rosa pluton with the orientation of the principal axes of the infinitesimal and finite strain ellipsoid according to the results of the kinematic model (long axis, *X*: black; intermediate axis, *Y*: purple; short axis, *Z*: red; arrows indicate the rotation of the principal axes with increasing finite deformation magnitude; left stereoplots for each case). Conceptual model 1, $W_k$ is the kinematic vorticity number. Because the principal axes of strain are not horizontal or vertical in this case, also the external map outline (red dashed lines) and $S_m$ patterns are compared with the principal (short and long) axes of the horizontal strain ellipse (right stereoplots for each case). (For interpretation of the references to colour in this figure legend, the reader is referred to the Web version of this article.)

kinematic study of the shear zones by calculating the oblique flow apophysis (see Fossen and Tikoff, 1998 for a detailed explanation). The divergence angles estimated in this work for the shear zone segments corresponding to both plutons are similar (blue double-headed vectors and blue shaded areas in Fig. 12). The common trend for both segments is oriented 157°±9°. This divergence angle implies that the shear zone would have acted during this period as a dextral transtensional structure with a strong predominance of the coaxial component (extension), except for segments oblique to the main structure, such as that of the Santa Rosa pluton. These oblique segments, where simple shear predominated, can be interpreted as R-type fractures (Riedel, 1929), synthetic to the main structure (Fig. 12).

During the Carboniferous, the brittle reactivation of several old basement structures and the nucleation of fault systems that cross-cut

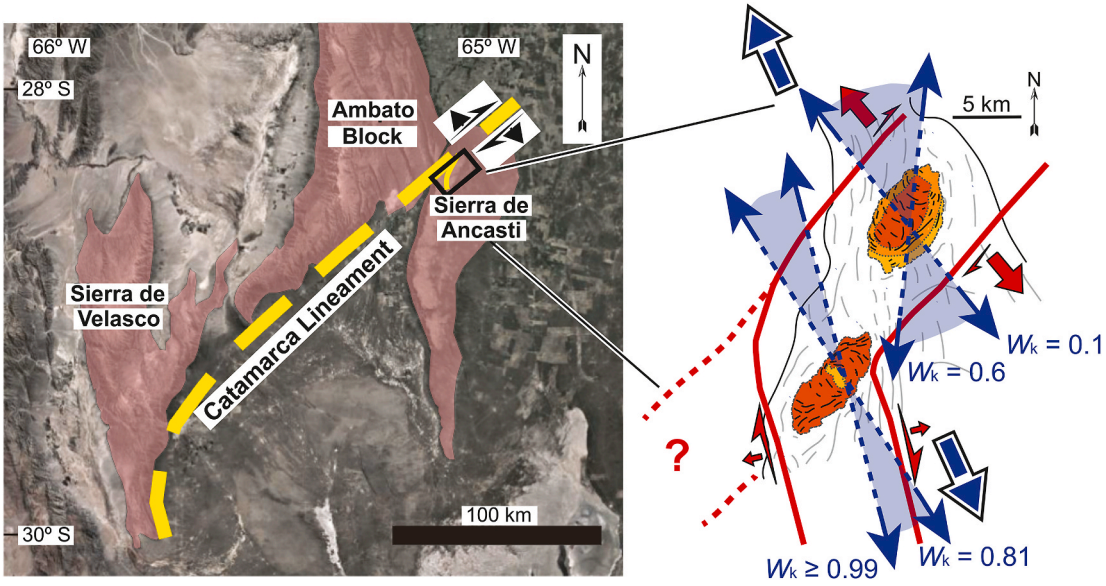


**Fig. 12.** Left: Sketch showing the location and approximate geometry of the Catamarca Lineament on a regional scale in the Eastern Sierras Pampeanas of Argentina (Baldis et al., 1975; Gutiérrez, 1999). Right: Results of the analytical kinematic model of the Catamarca Linement north of the Sierra de Ancasti (area of the Sauce Guacho and Santa Rosa plutons). The solid red lines indicate the trace of the curved shear zone defined in this work, and the dashed red lines show the possible extension of the shear zone towards the SW. The red arrows mark the kinematics (simple- and pure-shear components) deduced for each segment of the shear zone. The blue arrows and shaded areas correspond to the direction of divergence between the blocks separated by the shear zone in each segment. The large blue and white arrows indicate the average divergence direction in the studied area. (For interpretation of the references to colour in this figure legend, the reader is referred to the Web version of this article.)

metamorphic fabrics in an extensional/transtensional setting was proposed (Simpson et al., 2001; Whitmeyer, 2008; Limarino et al., 2013; Maffini et al., 2017; Acosta Nagle et al., 2022) and associated with a rapid exhumation (Enkelmann et al., 2014; Löbens et al., 2017; Dávila et al., 2021), intracontinental magmatism (Grosse et al., 2009; Coira et al., 2016; Dahlquist et al., 2010, 2014, 2015, 2021; Alasino et al., 2012, 2022; Acosta Nagle et al., 2022), polymetallic deposits (Hongn et al., 2010; Brodtkorb et al., 1999; Mutti et al., 2007; Maffini et al., 2017) and sedimentation in pull-apart basins (Limarino and Spalletti, 2006; Limarino et al., 2006; Astini et al., 2009; Gulbranson et al., 2010; Löbens et al., 2017).

The results obtained in this work show that the relative movement between basement blocks likely depended on the orientation of the reactivated structures in the different sectors of the Sierras Pampeanas in Carboniferous times. To the southeast (San Luis and Sierras de Córdoba ranges), the reactivated structures were dominantly subvertical N- to NW-striking (Fossen and Tykoff,1998; Brodtkorb et al., 1999; Mutti et al., 2007; Maffini et al. 2012, 2017; Maffini, 2015) with a maximum extension vector-oriented NNE-to NE, with the maximum shortening oriented WNW- to NW (Maffini et al., 2017). However, to the center-north in the Eastern Sierras Pampeanas (study area), the results obtained from this study show that the reactivation of the NE-SW brittle-ductile shear zone allowed the extension relative movement between blocks was NNW (around N157°E) (Fig. 12), similar to the extension direction determined for the Carboniferous Huaco Igneous Complex (354-345 Ma) in the center of the Sierra de Velasco (Macchioli-Grande et al., 2019). It is worth noting that the shear zone described in this work coincides with the NE part of the Catamarca Lineament trace (Baldis et al., 1975; Gutiérrez, 1999) (Fig. 12), a large structure that extends from the SE of the Sierra de Velasco and runs towards the NE along the limit between the Ambato Block and the Sierra de Ancasti. This regional lineament constitutes the north limit of the late Paleozoic Paganzo basin, a series of pull-apart depocenters and associated strike-slip deformation (Fernández Seveso and Tankard, 1995; Simpson et al., 2001; Chernicoff and Zappettini, 2007; Löbens et al., 2017). However, the information available so far on the kinematics of the Catamarca Lineament during the Paleozoic time is very limited.

## 8. Conclusions

The dynamics of small intrusive bodies emplaced in the middle-upper crust under conditions of brittle deformation are supposed to be dominated by the rapid processes of crystallization and cooling, where the influence of regional stresses on those processes is not easy to determine. However, the limited structural elements available at the surface, such as magmatic fabrics and refracted foliations of the metamorphic host rock in the vicinity of the igneous body, in addition to the geophysical study of the area, suggest clear control by a regional, arcuate transtensive structure in the emplacement of the studied plutons. We have used different methodologies of structural analysis to better constrain the kinematics of the shear zone that assisted the ascent and emplacement of the shallow reservoir, as an analytical model of monoclinic transpression/transtension, a method to obtain the initial orientation and the subsequent rotation of the extension fractures in the transtension regime and a transtensional folding model. According to our results, the different internal structural arrangement of both plutons can be explained in the context of the same stress regime, but determined by the arcuate shape of the Catamarca lineament, with a NNW-SSW-striking segment (Santa Rosa pluton area), where simple shear prevails (Wk $\gg$ 0.81 and probably $>$0.9), and a NE-SW striking segment (Sauce Guacho pluton area) with a predominance of pure shear (Wk between 0.1 and 0.6).

Furthermore, this work demonstrates that in the context of ancient tectonic stages where large structures and associated tectonites do not crop out, the kinematic study of plutons associated with these stages can reveal structural lineaments and endorse the determination of regional paleo-stresses.

## CRediT authorship contribution statement

**Ana Eugenia Acosta-Nagle:** Writing – review & editing, Writing – original draft, Visualization, Resources, Methodology, Investigation, Funding acquisition, Formal analysis, Conceptualization. **Juan Díaz-Alvarado:** Writing – review & editing, Writing – original draft, Visualization, Validation, Methodology, Investigation, Funding acquisition, Conceptualization. **Carlos Fernández:** Writing – review & editing, Writing – original draft, Supervision, Methodology, Formal analysis, Data curation, Conceptualization. **Rodolfo Christiansen:** Writing – original draft, Visualization, Resources, Project administration, Funding acquisition, Formal analysis. **Fernando Javier D'Eramo:** Resources, Investigation, Formal analysis, Conceptualization. **Lucio Pedro Pinotti:** Project administration, Funding acquisition, Formal analysis. **José Pablo López:** Supervision, Project administration, Funding acquisition, Formal analysis. **Laura Iudith Bellos:** Resources, Formal analysis.

## Declaration of competing interest

The authors declare that they have no known competing financial interests or personal relationships that could have appeared to influence the work reported in this paper.

## Acknowledgments

This study has been funded with PICT 2013–2015, CIUNT 26/G518, PICT 1754–2016, PICT 2707–2018 and PIUNT G709 projects.

## Data availability

All data included in this article are available for researchers.

## References

Aceñolaza, G., Aceñolaza, F., 2007. Insights in the Neoproterozoic–Early Cambrian Transition of NW Argentina: Facies, Environments and Fossils in the Proto-Margin of Western Gondwana, vol. 286. Geological Society, Special Publications, London, pp. 1–13.

Aceñolaza, F., Miller, H., Toselli, A., 1983. Geología de la Sierra de Ancasti. Münstersche Forschungen zur Geologie und Paläontologie 59, 1–372.

Aceñolaza, F.G., Miller, H., Toselli, A.J. (Eds.), 1990. El ciclo Pampeano en el Noroeste Argentino, vol. 4. Universidad Nacional de Tucumán, Serie Correlación Geológica, Tucumán, p. 388.

Aceñolaza, F., Toselli, A.J., 1977. Esquema geológico de la sierra de Ancasti, provincia de Catamarca. Acta Geol. Lilloana 14, 233–256.

Aceñolaza, F., Miller, H., Toselli, A.J., 1981. Geología de la sierra de Ancasti. Nuevos aportes al conocimiento geológico regional y estructural. Actas VIII Congreso Geológico Argentino 3, 75–88.

Aceñolaza, F.G., Miller, H., Toselli, A.J., 1988. The PuncoviscanaFormation (late Precambrian-early Cambrian). Sedimentology, Tectonometamorphic, history and age of the oldest rocks of NWArgentina. In: Bahlburg, En H. (Ed.), The Southern Central Andes. Lecture and Notes in Earth Sciences, pp. 25–37. Heidelberg.

Acosta Nagle, A.E., López, J.P., 2014. Geología y Petrología del Granito Tres Cerritos, extremo meridional de la Sierra de Quilmes y su relación con el magmatismo devónico-carbonífero de las Sierras Pampeanas. Rev. Asoc. Geol. Argent. 71 (3), 334–343.

Acosta Nagle, A.E., López, J.P., Pinotti, L., D'Eramo, F., 2017. Nuevas evidencias del metamorfismo estático $M_2$ en la Formación Ancasti, Sierras Pampeanas Noroccidentales, Argentina. Actas del XX Congreso Geológico Argentino, pp. 1–6. Tucumán.

Acosta-Nagle, A.E., Díaz-Alvarado, J., D'Eramo, F.J., López, J.P., Bellos, L.I., Pinotti, L.P., Gaeta Tassinari, C.C., Oliveros, V., Hanchar, J., 2022. Late Carboniferous intracontinental magmatism in the northernmost Sierras Pampeanas, Argentina: the case study of the Tres Cerritos pluton. J. S. Am. Earth Sci. 117, 103884.

Acosta-Nagle, A.E., Toselli, A., López, J.P., D'Eramo, F., Pinotti, L., Bellos, L.I., Díaz-Alvarado, J., 2024. Caracterización petrológica y estructural de la faja de cizalla El Alto, NE de la Sierra de Ancasti, Sierras Pampeanas Orientales de Argentina. Serie de Correlación Geológica, 40 (1), 5–16. https://doi.org/10.5281/zenodo.13738114.

Alasino, P.H., Dahlquist, J.A., Pankhurst, R.J., Galindo, C., Casquet, C., Rapela, C.W., Larrovere, M., Fanning, C.M., 2012. Early Carboniferous sub- to mid-alkaline magmatism in the Eastern Sierras Pampeanas, NW Argentina: a record of crustal growth by the incorporation of mantle-derived material in an extensional setting. Gondwana Res. 22, 992–1008.

Alasino, P.H., Paterson, S.R., Kirsch, M., Larrovere, M.A., 2022. The role of crustal thickness on magma composition in arcs: an example from the pre-Andean, South American Cordillera. Gondwana Res. 106, 191-10.
Allmendinger, R.W., Cardozo, N., Fisher, D.M., 2012. Structural Geology Algorithms: Vectors and Tensors. Cambridge University Press.
Aragón, E., D′ Eramo, F., Pinotti, L., Demartis, M., Tubía, J.M., Weinberg, R.F., Coniglio, J.E., 2019. Magma chamber growth models in the upper crust: a review of the hydraulic and inertial constraints. Geosci. Front. 10, 1211–1218. https://doi.org/10.1016/j.gsf.2018.10.005.
Aranguren, A., Tubía, J.M., Bouchez, J.L., Vigneresse, J.L., 1996. The Guitiriz granite, Variscan belt of northern Spain: extension-controlled emplacement of magma during tectonic escape. Earth Planet Sci. Lett. 139, 165–176.
Aranguren, A., Larrea, F.J., Carracedo, M., Cuevas, J., Tubía, J.M., 1997. The Los Pedroches batholith (southern Spain): polyphase interplay between shear zones in transtension and setting of granites. En. In: Bouchez, J.L., Hutton, D.H.W., Stephens, W.E. (Eds.), Granite: from Segregation of Melt to Emplacement Fabrics. Kluwer Academic Publishers, Dordrecht, pp. 215–229.
Astini, R.A., Martina, F., Ezpeleta, M., Dávila, F.M., Cawood, P.A., 2009. Chronology from rifting to foreland basin in the Paganzo basin (Argentina), and a reappraisal on the "Eo-and Neohercynian" tectonics along western Gondwana. In: Abstracts XII Congreso Geológico Chileno, vol. 179. Santiago S9-010.
Bachmann, O., Bergantz, G.W., 2004. On the origin of crystal-poor rhyolites: extracted from batholithic crystal mushes. J. Petrol. 45, 1565–1582.
Bachmann, O., Bergantz, G.W., 2008. The magma reservoirs that feed supereruptions. Elements 4, 17–21.
Báez, M.A., Fogliata, A., Hagemann, S., Santos, J.O., 2018. Magmatismo carbonífero en la Sierra de Ambato, Catamarca. Rev. Asoc. Geol. Argent. 75, 601–608.
Baldis, B.A., Viramonte, J., Salfity, J., 1975. Geotectónica de la comarca comprendida entre el Cratógeno Central Argentino y el borde austral de la Puna. 2° Congreso Iberoamericano de Geología Económica. Acta 4, 24–44. Buenos Aires.
Baldo, E.G., Stoessel, N., Murra, J.A., Dahlquist, J.A., 2008. Estructuras sedimentarias en los esquistos de la Formación Ancasti: reinterpretación de la evolución tectonotérmica. Actas del XVII Congreso Geológico Argentino 4, 1481–1482. Jujuy.
Becchio, R., Lucassen, F., Kasemann, S., Franz, G., Viramonte, J., 1999. Geoquímica y sistemática isotópica de rocas metamórficas del Paleozoico inferior. Noroeste de Argentina y Norte de Chile. Acta Geol. Hisp. 34, 273–299.
Bouchez, J.L., Guillet, P., Chevalier, F., 1981. Structures d'ecoulementliees a la mise en place du granite de Guerande (Loire-Atlanticue, France). Bull. Soc. Geol. Fr. 23, 387–399.
Bouchez, J.L., Delas, C., Gleizes, G., Nédélec, A., y Cuney, M., 1992. Submagmatic microfractures in granites. Geology 20 (1), 35–38.
Bouchez, J.L., 1997. Granite is never isotropic: an introduction to ASM studies of granitic rocks. In: Bouchez, J.L., Hutton, D.H.W., Stephens, W.E. (Eds.), Granite: from Segregation of Melt to Emplacement Fabrics, Petrology and Structural Geology. Kluwer, Dordrecht, pp. 95–112.
Brodtkorb, M.K., Fernández, R. y, Pezzutti, N., 1999. Yacimientos de wolframio asociados a metavolcanitas y metasedimentitas, San Luis. In: En Zappettini, E. (Ed.), Recursos Minerales de la República Argentina. Instituto de Geología y Recursos Minerales, vol. 35. SEGEMAR, Anales, Buenos Aires, pp. 323–335.
Brown, M., Solar, G.S., 1998. Shear-zone systems and melts: feedback relations and self-organization in orogenic belts. J. Struct. Geol. 20, 211–227.
Brun, J.P., Pons, J., 1981. Strain patterns of pluton emplacement in a crust undergoing non-coaxial deformation, Sierra Morena, Southern Spain. J. Struct. Geol. 3, 219–229.
Büttner, S.H., Glodny, J., Lucassen, F., Wemmer, K., Erdmann, S., Handler, R., Franz, G., 2005. Ordovician metamorphism and plutonism in the Sierra de Quilmes metamorphic complex: Implications for the tectonic setting of the northern Sierras Pampeanas (NW Argentina). Lithos 83, 143–181.
Calcagno, P., Chiles, J.P., Courrioux, G., Guillen, A., 2008. Geological modelling from field data and geological knowledge Part I. Modelling method coupling 3D potential field interpolation and geological rules. Phys. Earth Planet. In. 171, 147–157.
Campbell, I.H., Turner, J.S., 1989. The influence of viscosity onfountains in magma chambers. J. Petrol. 30 (4), 885–923.
Castro Dorado, A., 1989. Petrografia Básica. Texturas, clasificación y nomenclatura de rocas. Editorial Paraninfo SA, Madrid, p. 143.
Cardozo, N., Allmendinger, R.W., 2013. Spherical projections with OSXStereonet. Computers & Geosciences 51, 193–205.
Castro, A., 1986. Structural pattern and ascent model in the Central Extremadura batholith, Hercynian belt, Spain. J. Struct. Geol. 8, 633–645.
Chernicoff, C.J., Zappettini, E.O., 2007. La cuenca paleozoica de Arizona, sudeste de San Luis, Argentina: extensión austral de la cuenca de Paganzo. Rev. Asoc. Geol. Argent. 62 (2), 321–324.
Christiansen, R., Morosini, A., Enriquez, E., Muñoz, B., Lince Klinger, F., Martinez, M.P., Ortiz Suárez, A., Kostadinoff, J., 2019. 3D litho-constrained inversion model of southern Sierra Grande de San Luis: New insights into the Famatinian tectonic setting. Tectonophysics 756, 1–24.
Clark, D.A., 1999. Magnetic petrology of igneous intrusions: implications for exploration and magnetic interpretation. Explor. Geophys. 30, 5–26.
Clark, D.A., 1997. Magnetic petrophysics and magnetic petrology: aids to geological interpretation of magnetic surveys. AGSO J. Aust. Geol. Geophys. 17, 83–104.
Clemens, J.D., 1998. Observations on the origins and ascent mechanisms of granitic magmas. J. Geolo.Soci. Lon. 155, 843–851.
Clemens, J.D., Mawer, C.K., 1992. Granitic magma transport by fracture propagation. Tectonophysics 204, 339–360.
Coira, B., Cisterna, C., Ulbrich, H.H., Cordani, U.G., 2016. Extensional carboniferous magmatism at the western margin of Gondwana: las Lozas valley, Catamarca, Argentina. Andean Geol. 43, 105–126.
Courrioux, G., 1982. Exemple de mise en place d'un leucogranite pendant le fonctionnement d'une zone de cisaillement: le granite hercynien de Puentedeume (Galice, Espagne). Bullin Society of Geology of France 12, 301–307.
Dahlquist, J.A., Alasino, P.H., Eby, G.N., Galindo, C., Casquet, C., 2010. Fault controlled Carboniferous A-type magmatism in the proto-Andean foreland (Sierras Pampeanas, Argentina): geochemical constraints and petrogenesis. Lithos 115, 65–81.
Dahlquist, J.A., Pankhurst, R.J., Gaschnig, R.M., Rapela, C.W., Casquet, C., Alasino, P.H., Galindo, C., Baldo, E.G., 2013. Hf and Nd isotopes in Early Ordovician to Early Carboniferous granites as monitors of crustal growth in the Proto-Andean margin of Gondwana. Gondwana Res. 23, 1617–1630.
Dahlquist, J.A., Alasino, P.H., Bello, C., 2014. Devonian f-rich peraluminous A-type magmatism in the proto-Andean foreland (Sierras Pampeanas, Argentina): geochemical constraints and petrogénesis from the western-central region of the Achala batholith. Mineral. Petrol. 108, 391–417.
Dahlquist, J.A., Pankhurst, R.J., Rapela, C.W., Basei, M.A.S., Alasino, P.H., Saavedra, J., Baldo, E.G., Murra, J., Costa Campos Neto, M., 2015. The Capilla del Monte pluton, Sierras de Córdoba, Argentina: the easternmost Early Carboniferous magmatism in the pre-Andean SW Gondwana margin. Int. J. Earth Sci. 105, 1287–1305.
Dahlquist, J.A., Alasino, P.H., Basei, M.A.S., Morales Camera, M., Macchioli Grande, M., da Costa Campos Neto, M.C., 2018. Petrological, geochemical, isotopic, and geochronological constraints for the Late Devonian - early Carboniferous magmatism in SW Gondwana (27∘-32∘LS): an example of geodynamic switching. Int. J. Earth Sci. 107, 2575–2603.
Dahlquist, J.A., Morales Cámera, M.M., Alasino, P.H., Pankhurst, R.J., Basei, M.A.S., Rapela, C.W., Moreno, J.A., Baldo, E.G., Galindo, C., 2021. A review of the Devonian-Carboniferous magmatism in the central region of Argentina, pre-Andean margin of SW Gondwana. Earth Sci. Rev. 221, 103781.
Daly, R.A., 1933. Igneous Rocks and the Depths of the Earth. McGraw-Hill, New York.
Dávila, F.M., Martina, F., Parra, M., Ávila, P., 2021. Effects of uplift on Carboniferous exhumation and mountain glaciations in pericratonic areas of SW Gondwana, central Argentina. Tectonics 40. https://doi.org/10.1029/2021TC006855.
D'Eramo, F.J., Pinotti, L., Tubia, J.M., Vegas, N., Aranguren, A., Tejero, R., Goméz, D., 2006. Coalescence of lateral spreading magma ascending through dykes: a mechanism to form a granite canopy (El Hongo pluton, Sierras Pampeanas, Argentina). J. Geolo.Soci. Lon. 163, 881–892.
D'Eramo, F., Tubía, J.F., Pinotti, L., Vegas, N., Coniglio, J., Demartis, M., Arangueren, A., Basei, M., 2013. Granite emplacement by crustal boudinage: example of the Calmayo and El Hongo plutons (Córdoba, Argentina). Terra. Nova 1–8. https://doi.org/10.1111/ter.12053, 0.
De Saint Blanquat, M., Tikoff, B., Teyssier, C., Vigneresse, J., 1998. Tranpressional kinematics and magmatic arcs. In: Holdsworth, R., Strachan, R., Dewey, J. (Eds.), Continental Transpressional and Transtensional Tectonics, vol. 135. Geological Society of London, Special Publication, pp. 327–340.
De Saint Blanquat, M., Horsman, E., Habert, G., Morgan, S., Vanderhaeghe, O., Law, R., Tikoff, B., 2011. Multiscale magmatic cyclicity, duration of pluton construction, and the paradoxical relationship between tectonism and plutonism in continental arcs. Tectonophysics 500, 20–33.
Díaz-Alvarado, J., Fernández, C., Díaz Azpiroz, M., Castro, A., Moreno-Ventas, I., 2012. Fabric evidence for granodiorite emplacement with extensional shear zones in the Variscan Gredos massif (Spanish Central System). J. Struct. Geol. 42, 74–90. https://doi.org/10.1016/j.jsg.2012.06.012.
Durand, F.R., 1996. La transición Precámbrico-Cámbrico en el sur de Sudamérica. In: Aceñolaza, B.Baldis yF. (Ed.), Early Paleozoic Evolution in NW Gondwana, vol. 12. Universidad Nacional de Tucumán, Argentina, Serie Correlación Geológica, pp. 195–205.
Enkelmann, E., Ridgway, K.D., Carignano, C., Linnemann, U., 2014. A thermochronometric view into an ancient landscape: tectonic setting, development, and inversion of the Paleozoic eastern Paganzo basin, Argentina. Lithosphere 6, 93–107.
Fernández, C., Castro, A., 1999. Pluton accomodation at high strain rates in the upper continental crust. The example of the Central Extremadura batholith, Spain. J. Struct. Geol. 21, 1143–1149.
Fernández, C., Castro, A., 2018. Mechanical and structural consequences of magma differentiation at ascent conduits: a possible origin for some mafic microgranular enclaves in granites. Lithos 320–321, 49–61. https://doi.org/10.1016/j.lithos.2018.09.004.
Fernández, C., Díaz Azpíroz, M., 2009. Triclinic transpression zones with inclined extrusion. J. Struct. Geol. 31, 1255–1269.
Fernández, C., Díaz Azpíroz, M., 2022. Extension structures as kinematic indicators in monoclinic transpression and transtension zones. J. Struct. Geol. 161, 104639.
Fernández-Seveso, F., Tankard, A.J., 1995. Tectonics and stratigraphy of the late paleozoic Paganzo basin of western Argentina and its regional implications. In: Tankard, A.J., Suárez Soruco, R., Welsink, J. (Eds.), Petroleum Basins of South America, vol. 62. American Association of Petroleum Geologists, Memoir, pp. 285–301.
Fossen, H., Tikoff, B., 1998. Extended models of transpression and transtension, and application to tectonic settings. In: Holdsworth, R.E., Strachan, R.A., Dewey, J.E. (Eds.), Continental Transpressional and Transtensional Tectonics, vol. 135. Geological Society of London, Special Publications, pp. 15–33.
Fossen, H., Teyssier, C., Whitney, D.L., 2013. Transtensional folding. J. Struct. Geol. 56, 89–102.
Grosse, P., Sardi, F.G., 2005. Geología de los granitos Huaco y Sanagasta, sector centrooriental de la Sierra de Velasco, La Rioja. En. In: Aceñolaza, F.G., Aceñolaza, G.F., Hünicken, M., Rossi, J.N. y, Toselli, A.J. (Eds.), Simposio Bodenbender, Serie de Correlación Geológica, pp. 221–238. Tucumán.

Grosse, P., Söllner, F., Báez, M.A., Toselli, A.J., Rossi, J.N., De La Rosa, J.D., 2009. Lower Carboniferous post-orogenic granites in central-eastern Sierra de Velasco, Sierras Pampeanas, Argentina: U-Pb monazite geochronology, geochemistry and Sr-Nd isotopes. Int. J. Earth Sci. 98, 1001–1025.

Guillen, A., Calcagno, P., Courrioux, G., Joly, A., Ledru, P., 2008. 3D realistic modelling of geology from field data and geological knowledge, part II -modelling validation using of gravity and magnetic data inversion. Phys. Earth Planet. In. 171, 158–169.

Guillet, P., Bouchez, J.L., Vigneresse, J.L., 1985. Le complèxe granitique de Plouaret: mise en evidence structurale et gravimétrique de diapers emboite's. Bull. Soc. Geol. Fr. 8, 503–513.

Gulbranson, E.L., Montañez, I.P., Schmitz, M.D., Limarino, C.O., Isbell, J.L., Marenssi, S. A., Crowley, J.L., 2010. High-precision U-Pb calibration of Carboniferous glaciation and climate history, Paganzo Group, NW Argentina. Geol. Soc. Am. Bull. 122, 1480–1498.

Gutiérrez, A.A., 1999. Tectonic geomorphologyof the Ambato block (Northwestern Pampeanas mountain ranges, Argentina). FourthInternational Symposium on Andean Geodynamics, pp. 307–310. Göttingen.

Hecht, L., Vigneresse, J.L., 1999. A multidisciplinary approach combining geochemical, gravity and structural data: implications for pluton emplacement and zonation. In: Castro, A., Fernández, C., Vigneresse, J.L. (Eds.), Understanding Granites: Integrating New and Classical Techniques, vol. 168. Geological Society of London, Special Publication, pp. 95–110.

Hinze, W.J., 2003. Bouguer reduction density, why 2.67? Geophysics 68 (5), 1559–1560.

Hinze, W.J., Aiken, C., Brozena, J., Coakley, B., Dater, D., Flanagan, G., Forsberg, R., Hildenbrand, T., Keller, G.R., Kellogg, J., Plouff, D., Ravat, D., Roman, D., Urrutia-Fucugauchi, J., Véronneau, M., Webring, M., Winester, D., 2005. New standards for reducing gravity data: the North American gravity database. Geophysics 70, J25–J32.

Hongn, F., Ferreira, L., Morello, O., Rubinstein, N., Kirschbaum, A., Guidi, F., Anesa, J., 2010. Control estructural sobre el plutón Los Ratones y la mineralización de uranio en la sierra de Fiambalá, Sierras Pampeanas, Catamarca. Rev. Asoc. Geol. Argent. 67 (4), 545–561.

Hutton, D.H.W., 1982. A tectonic model for the emplacement of the main Donegal granite, NW Ireland. Journal of Geological Society of London 139, 615–631.

Hutton, D.H.W., 1988. Granite emplacement mechanisms and tectonic controls: inferences from deformation studies. Trans. R. Soc. Edinb. Earth Sci. 79, 245–255.

Hutton, D.H.W., 1992. Granite sheeted complexes: evidence for the dyking ascent mechanism. Trans. R. Soc. Edinb. Earth Sci. 83, 377–382.

Hutton, D.H.W., 1997. Syntectonic granites and the principle of effective stress: a general solution to the space problem? In: Bouchez, J.L., Stephens, W.E., Hutton, D.H.W. (Eds.), Granite: from Melt Segregation to Emplacement Fabrics. Kluwer Academic Publishers, pp. 189–197.

Hutton, D.H.W., Reavy, R.J., 1992. Strike-slip tectonics and granite petrogenesis. Tectonics 11, 960–967.

Hutton, D.H.W., Depster, T.J., Brown, P.E., Becker, S.D., 1990. A new mechanism of granite emplacement: intrusion in active extensional shear zones. Nature 343, 452–455.

Ibañez, R., 1978. Contribución al conocimiento geológico del extremo norte de la Sierra de Ancasti, Depto. El Alto, provincia de Catamarca. Seminario. Facultad de Ciencias Naturales e I.M.L. Universidad Nacional de Tucumán. Inédito.

Ishihara, S., 1977. The magnetite-series and ilmenite-series granitic rocks. Min. Geol. 27, 293–305.

Isles, D.J., Rankin, L.R., 2013. Geological Interpretation of Aeromagnetic Data. Australian Society of Exploration Geophysicists, Perth.

Jêzek, P., 1990. Análisis sedimentológico de la Formación Puncoviscana entre Tucumán y Salta. In: Aceñolaza, F., Miller, H., Toselli, A.J. (Eds.), El Ciclo Pampeano en el noroeste argentino, vol. 4. Serie Correlación Geológica, Tucumán, pp. 9–36.

Kamb, W.B., 1959. Petrofabric observations from Blue Glacer, Washington, in relation to theory and experiment. J. Geophys. Res. 64, 1908–1909.

Knüver, M., 1983. Dataciones radimétricas de rocas plutónicas y metamórficas. In: En Aceñolaza, F.G., Miller, H. y, Toselli, A. (Eds.), Geología de la Sierra de Ancasti, Munstersche Forschungen zur Geologie und Palaontologie, vol. 59, pp. 201–218.

Knüver, M., Reissinger, M., 1981. The plutonic and metamorphic history of the sierra de Ancasti (Catamarca province, Argentina) ZBL. Geologisch und Paläontologie 1, 285–297.

Lafehr, T.R., 1991. An exact solution for the gravity curvature. Bullard B) correction Geophysics 56, 1179–1184.

Larrovere, M.A., de los Hoyos, C.R., Toselli, A.J., Rossi, J.N., Basei, M.A.S., Belmar, M.E., 2011. High T/P evolution and metamorphic ages of the migmatitic basement of northern Sierras Pampeanas, Argentina: characterization of a mid-crustal segment of the Famatinian belt. J. S. Am. Earth Sci. 31, 279–297.

Limarino, C.O., Spalletti, L.A., Colombo Piñol, F., Ciccioli, P.L., 2013. Dynamics of the Valle Fértil Lineament during the Late Paleozoic Based on Petrofacies Analysis (Northwest Argentina), vol. 1. Bolletino di Geofisica Teoretica ed Applicata, p. 24.

Limarino, C., Tripaldi, A., Marenssi, S., Fauqué, L., 2006. Tectonic, sea-level, and climatic controls on Late Paleozoic sedimentation in the western basins of Argentina. J. S. Am. Earth Sci. 22 (3), 205–226.

Limarino, C., Spalletti, L., 2006. Paleogeography of the upper Paleozoic basins of southern South America: an overview. J. S. Am. Earth Sci. 22 (3), 134–155.

Lira, R., Kirschbaum, A.M., 1990. Geochemical evolution of granites from the achala batholith of the sierras pampeanas, Argentina. Geol. Soc. Am. Spec. Pap. 241, 67–76. https://doi.org/10.1130/SPE241-p67.

Llambias, E.J., 2008. Geología de los cuerpos ígneos. Asociación Geológica Argentina, Serie B Didáctica y Complementaria N° 29, Serie de Correlación Geológica. Instituto Superior de Correlación Geológica 15, 121–123. Buenos Aires.

Llambías, E.J., Sato, A.M., Ortiz Suárez, A., Prozzi, C., 1998. The granitoids of the sierra de San Luis. In: Pankhurst, R.J., Rapela, C.W. (Eds.), The Proto-Andean Margin of Gondwana, vol. 142. Geological Society of London, Special Publications, London, pp. 325–341.

Löbens, S., Oriolo, S., Benowitz, J., Wemmer, K., Layer, P., Siegesmund, S., 2017. Late Paleozoic deformation and exhumation in the Sierras Pampeanas (Argentina): $^{40}Ar/^{39}Ar$-feldspar dating constraints. J. Earth Sci. 106, 1991–2003.

López de Luchi, M.G., Rapalini, A.E., Siegesmund, S., Steeken, A., 2012. Application of magnetic fabrics to the emplacement and tectonic history of Devonian granitoids in central Argentina. Geol.Soci.Lon. 238, 447–474.

López de Luchi, M.G., Siegesmund, S., Wemmer, K., Nolte, N., 2017. Petrogenesis of postcollisional Middle Devonian monzonitic to granitic magmatism of the Sierra de San Luis, Argentina. Lithos 288, 191–213.

Macchioli Grande, M., Alasino, P.H., Rocher, S., Larroverea, M.A., Urana, G.M., Reinoso Carbonella, V., Moreno, G., 2019. Thermal evolution of upper crustal magmatic systems from the Sierra de Velasco, NW Argentina. J. Struct. Geol. 118, 1–20.

Maffini, M.N., 2015. Estudio petro-estructural, mineralógico y metalogenético de depósitos vetiformes mesotermales (Pb-Zn-Cu-Ag-Au) emplazados en el basamento metamórfico de la Sierra de Comechingones, en proximidad a cuerpos ígneos plutónicos, Sierras PampeanasOrientales. Unpublished PhD Thesis, Universidad Nacional de Río Cuarto, Río Cuarto, p. 284.

Maffini, M.N., Coniglio, J.E., Demartis, M., D'Eramo, F.J., Pinotti, L.P., Bin, I. y, Petrelli, H.A., 2012. Vetas mesotermales de Pb-Zn-Ag-Au emplazadas al este del Batolito Cerro Áspero, Sierra de Comechingones, Córdoba. Ser. Correlación Geol. 28 (2), 93–106.

Maffini, M.N., Wemmer, K., Radice, S., Oriolo, S., D'Eramo, F., Coniglio, J., Demartis, M., Pinotti, L., 2017. Polymetallic (Pb-Zn-Cu-Ag±Au) vein-type deposits in brittle-ductile transtensional shear zones, Eastern Sierras Pampeanas (Argentina): age constraints and significance for the Late Paleozoic tectonic evolution and metallogenesis. Ore Geol. Rev. 89, 668–682.

Marcotte, S.B., Klepeis, K.A., Clarke, G.L., Gehrels, G., Hollis, J.A., 2005. Intra-arc transpression in the lower crust and its relationship to magmatism in a Mesozoic magmatic arc. Tectonophysics 407, 135–163.

McInerney, P., Guillen, A., Courrioux, G., Calcagno, P., Lees, T., 2005. Building 3D geological models directly from the data? A new approach applied to broken hill, Australia; digital mapping techniques '05; workshop proceedings. Open File Rep. U. S. Geol. Surv. 1428, 119–130.

Miller, H. y, Willner, A., 1981. The Sierra de Ancasti (Catamarca Province), an example of polyphase deformation of Lower Paleozoic age in the Pampean Ranges. Zentralblatt für Geologie und Paläontologie I (3/4), 272–284.

Miller, H., Aceñolaza, F.G., Toselli, A.J., 1978. Reseña estructural de la Sierra de Ancasti. Acta Geol. Lilloana 15, 31–39.

Miller, C.F., Furbish, D.J., Walker, B.A., Claiborne, L.L., Koteas, G.C., Bleick, H.A., Miller, J.S., 2011. Growth of plutons by incremental emplacement of sheets in crystal-rich host: evidence from Miocene intrusions of the Colorado River region, Nevada, USA. Tectonophysics 500, 65–77.

Miró, R., Gaido, F., Candiani, J. y, Aimar, C., 2004. Hoja geológica Recreo, 2966-IV, 1: 250.000. Instituto de Geología y Recursos Minerales. SEGEMAR, p. 84.

Murphy, D.C., 1987. Suprastructure/infrastructure transition. east-central Cariboo Mountains, British Columbia: geomctn. kinematics. and tectomc implication. J. Struct.Geol. 132, 281–295.

Murra, J.A., Baldo, E.G., Galindo, C., et al., 2011. Sr, C and O isotope composition of marbles from the Sierra de Ancasti, Eastern Sierras Pampeanas, Argentina: age and constraints for the Neoproterozoic–Lower Paleozoic evolution of the proto-Gondwana margin. Geol. Acta 9, 79–92.

Mutti, D., Di Marco, A., Geuna, S., 2007. Depósitos polimetálicos en el orógeno famatiniano de las Sierras Pampeanas de San Luis y Córdoba: Fluidos, fuentes y modelos de emplazamiento. Rev. Asoc. Geol. Argent. 62 (1), 44–61.

Omarini, R., Sureda, R., Götze, H., Seilacher, A. y, Pfüger, F., 1999. Puncoviscana folded belt in northwestern Argentina: testimony of Late Proterozoic Rodinia fragmentation and pre-Gondwana collisional episodes. Int. J.Eatrh Sci. 88, 76–97.

Oriolo, S., Gómez, A.N.L., Maffini, M.N., Oyhantçabal, P., Morales Demarco, M., Vargas Perucca, M.S., Bastías Torres, M.V., Rubinstein, N.A., 2024. Transtension, brittle-ductile shear zones and hydrothermal ore deposits: towards quantitative structural and kinematic models. J. Struct. Geol. 185. https://doi.org/10.1016/j.jsg.2024.105173.

Passchier, C.W., 1998. Monoclinic model shear zones. J. Struct. Geol. 20, 1121–1137.

Petford, N., Cruden, A.R., McCaffrey, K.J.W., Vigneresse, J.L., 2000. Dynamics of granitic magma formation, transport and emplacement in the Earth's crust. Nature 408, 669–673.

Pinotti, L., D'Eramo, F., 2008. Estructuras de los Cuerpos ígneos. En Geología de los cuerpos ígneos. Asociación Geológica Argentina, Serie B Didáctica y Complementaria N° 29, Serie de Correlación Geológica. Instituto Superior de Correlación Geológica 15, 121–123. Buenos Aires.

Pinotti, L.P., Coniglio, J., Esparza, A.M., D'Eramo, F.J., Llambías, E.J., 2002. Nearly circular plutons emplaced by stoping at shallow crustal levels. Cerro Aspero Batholith, Sierras Pampeanas de Córdoba, Argentina. J. S. Am. Earth Sci. 15, 251–265.

Pinotti, L.P., Tubía, J.M., D'Eramo, F., Vegas, N., Sato, A.M., Coniglio, J., Aranguren, A., 2006. Structural interplay between plutons during the construction of a batholith (Cerro Áspero batholith, Sierras de Córdoba, Argentina). J. Struct. Geol. 28, 834–849.

Rapela, C.W., 1976. El basamento metamorfico de la región de Cafayate, Provincia de Salta. Aspectos petrologicos y geoquimicos. Rev. Asoc. Geol. Argent. 31, 203–222.

Rapela, C., Pankhurst, R., Casquet, C., Baldo, E., Saavedra, J., Galindo, C., 1998. Early evolution of the proto-andean margin of south America. Geology 26 (8), 707–710.

Rapela, C.W., Pankhurst, R.J., Casquet, C., Fanning, C.M., Baldo, E.G., González-Casado, J.M., Galindo, C., Dahlquist, J., 2007. The Río de la Plata craton and the assembly of SW Gondwana. Earth Sci. Rev. 83 (1–2), 49–82.

Riedel, W., 1929. Zur mechanik geologischer brucherscheinungen. - zentralblat fuer mineralogie. Geol. Palaeontol. 354–368.

Rodríguez, C., Castro, A., 2017. Silicic magma differentiation in ascent conduits. Experimental constraints. Lithos 272–273, 261–277.

Rodríguez, C., Castro, A., 2018. Origins of mafic microgranular enclaves and enclave swarms in granites: field and geochemical relations. Geol. Soc. Am. Bull. 131 (3–4), 635–660.

Rossi de Toselli, J.N., Toselli, A.J., Toselli, G.A., 1976. Migmatizacion y metamorphismo en el basamento de la Sierra de Quilmes, al oeste de Colalao del Valle, Provincia de Tucumán, Argentina. Rev. Asoc. Geol. Argent. 31, 83–94.

Sardi, F.G., Vignal-Lelarge, M.L., Iriarte, M.E., Soares, C.J., 2023. Geological and geochronological implications of U-Pb dating in apatite from the Late Devonian/Early Carboniferous Sauce Guacho granite, Sierra de Ancasti, NW Argentina. J. S. Am. Earth Sci. https://doi.org/10.2139/ssrn.4530684.

Siegesmund, S., Steenken, A., López de Luchi, M.G., Wemmer, K., Hoffmann, A., Mosch, S., 2004. The Las Chacras–Potrerillos batholith (Pampean Ranges, Argentina): structural evidence, emplacement and timing of the intrusion. Int. J. Earth Sci. 93, 23–43.

Simpson, C., Whitmeyer, S.J., De Paor, D.G., Gromet, L.P., Miró, R., Krol, M.A., Short, H., 2001. Sequential ductile to brittle reactivation of major fault zones along the accretionary margin of Gondwana. In: Holdsworth, R.E., Strachan, R.A., Magloughlin, J.F., Knipe, R.J. (Eds.), The Nature and Tectonic Significance of Fault Zone Weakening, vol. 186. Geological Society of London, Special Publication, pp. 233–255.

Smithson, S.B., 1971. Densities of metamorphic rocks. Geophysics 36, 690–694.

Stevenson, C.T.E., Hutton, D.H.W., Price, A.R., 2008. The trawenagh bay granite and a new model for the emplacement of the donegal batholith. Trans. R. Soc. Edinb. Earth Sci. 97, 455–477.

Stuart-Smith, P.G., Miró, R., Sims, J.P., Pieters, P.E., Lyons, P., Camacho, A., Skirrow, R. G., Black, L.P., 1999. Uranium–lead dating of felsic magmatic cycles in the southern Sierras Pampeanas, Argentina: implications for the tectonic development of the proto-Andean Gondwana margin. In: Ramos, V.A., Keppie, J.D. (Eds.), Laurentia–Gondwana Connections before Pangea, vol. 336. Geological Society of America, Special Publication, pp. 87–114.

Tobish, O.T., Paterson, S.R., 1990. The Yarra granite: an intradeformational pluton associated with ductile thrusting, Lachlan Fold Belt, southeastern Australia. Geol. Soc. Am. Bull. 102, 693–703.

Tommasi, A., Vauchez, A., Fernandes, L.A.D., y Porcher, C.C., 1994. Magma-assisted strain localization in an orogen-parallel transcurrent shear zone of southern Brazil. Tectonics 2, 421–437.

Toselli, A., Rossi de Toselli, J.N., 2018. Granitoides devonico - carboniferos de las sierras pampeanas noroccidentales y sus relaciones con la fuente y el ambiente tardio - a post - orogenico del ciclo Famatiniano. Ser. Correlación Geol. 35 (2), 37–66.

Toselli, A.J., Rossi, J.N., Basei, M.A.S., 2014. Geología e interpretación petrológica de los granitos y pegmatitas de la Sierra de Mazán, La Rioja, Argentina. Ser. Correlación Geol. 30, 7–20.

Toselli, A.J., Rossi, J.N., Rapela, C.W., 1978. El basamento metam'orfico de la Sierra de Quilmes, Argentina. Rev. Asoc. Geol. Argent. 33, 105–121.

Toselli, A.J., Rossi, J.N., Basei, M.A.S., Passarelli, C.R., 2011. Petrogenesis of Upper-Paleozoic post-collisional peraluminous leucogranites, Sierra de Ancasti, northwest Argentina. Neues Jarhbuch für Geologisch und Paläontologisch Abhandlungen 236, 129–147.

Truesdell, C.A., 1953. Two measures of vorticity. J. Rational Mechanics and Mechanical Analysis 2, 173–217.

Turner, J.C.M., 1960. Estratigrafía de la Sierra de Santa Victoria y adyacencias, vol. 41. Boletín de la Academia Nacional de Ciencias, pp. 163–196.

Valentine, G.A., 1992. Magma chamber dynamics. En: Enciclopedia of Earth System Science. Academic Press, pp. 1–17.

Vegas, N., Aranguren, A., Cuevas, J., Tubía, J.M., 2001. Variaciones en los mecanismos de emplazamiento de los granitos del eje Sanabria-Viana do Bolo (Macizo Ibérico, España). Bol. Geol. Min. 112 (3), 79–88.

Verdechia, S.O., Reche, J., Baldo, E.G., Segovia-Díaz, E., Martínez, F.J., 2012. Staurolite porphyroblast controls on local bulk compositional and microstructural changes during decompression of a St–Bt–Grt–Crd–And schist (Ancasti metamorphic complex, Sierras Pampeanas, W Argentina). J. Metamorph. Geol. https://doi.org/10.1111/jmg.12003.

Vigneresse, J.L., 1995. Control of granite emplacement by regional deformation. Tectonophysics 249, 173–186.

Vigneresse, J.L., 2004. A new paradigm for granite generation. Trans. R. Soc. Edinb. Earth Sci. 95, 11–22.

Vigneresse, J.L., Barbey, P., Cuney, M., 1996. Rheological transitions during partial melting and crystallization with application to felsic magma segregation and transfer. J. Petrol. 37, 1579–1600.

Willner, A.P., 1983. Evolución metamórfica. In: Aceñolaza, F.G., Miller, H. y, Toselli, A. (Eds.), La geología de la Sierra de Ancasti, vol. 59. Munster, Munstersche Forschungen zur Geologie und Paleontologie, pp. 189–200.

Willner, A.P., Toselli, A.J., Basán, C., Vides de Bazán, M.E., 1983. Rocas metamórficas. In: Acenñolaza, F.G., Miller, H. y, Toselli, A. (Eds.), La geología de la Sierra de Ancasti, vol. 59. Munster, Munstersche Forschungen zur Geologie und Paleontologie, pp. 31–78.

Whitney, D.L., y Evans, B.W., 2010. Abbreviations for names of rock-forming minerals. Am. Mineral. 95, 185–187.

Whitmeyer, S., 2008. Dating fault fabrics using modern techniques of $^{40}Ar/^{39}Ar$ thermochronology: evidence for Paleozoic deformation in the Eastern Sierras Pampeanas, Argentina. Journal of the Virtual Explorer, Electronic Edition 30. https://doi.org/10.3809/jvirtex.2008.00207 paper 3.

Žák, J., Holub, F.V., Kachlík, V., 2006. Magmatic stoping as an important emplacement mechanism of variscan plutons: evidence from roof pendants in the central bohemian plutonic complex (bohemian massif). Int. J. Earth Sci. 95, 771–789. https://doi.org/10.1007/s00531-006-0076-8.

Zappettini, E.O., 1999. Depósitos de fluorite del Distrito El Alto, Catamarca. En Recursos Minerales de la República Argentina. In: Zappettini, E.O. (Ed.), Instituto de Geología y Recursos Minerales, SEGEMAR. Anales, vol. 35, pp. 655–656. Buenos Aires.